SPIRITS 15c and SPIRITS 14buu: Two Obscured Supernovae in the Nearby Star-forming Galaxy IC 2163

The Astrophysical Journal, 837:167 (19pp), 2017 March 10 https://doi.org/10.3847/1538-4357/aa618f

SPIRITS 15c and SPIRITS 14buu: Two Obscured Supernovae in the Nearby Star-forming Galaxy IC 2163

Jacob E. Jencson[1,13], Mansi M. Kasliwal[1], Joel Johansson[2], Carlos Contreras[3], Sergio Castellón[3], Howard E. Bond[4,5], Andrew J. Monson[4], Frank J. Masci[6], Ann Marie Cody[7], Jennifer E. Andrews[8], John Bally[9], Yi Cao[1], Ori D. Fox[5], Timothy Gburek[10], Robert D. Gehrz[10], Wayne Green[9], George Helou[6], Eric Hsiao[11], Nidia Morrell[3], Mark Phillips[3], Thomas A. Prince[1], Robert A. Simcoe[12], Nathan Smith[8], Samaporn Tinyanont[1], and Robert Williams[5]
[1] Cahill Center for Astronomy and Astrophysics, California Institute of Technology, Pasadena, CA 91125, USA; jj@astro.caltech.edu
[2] Benoziyo Center for Astrophysics, Weizmann Institute of Science, 76100 Rehovot, Israel
[3] Las Campanas Observatory, Carnegie Observatories, Casilla 601, La Serena, Chile
[4] Dept. of Astronomy & Astrophysics, Pennsylvania State University, University Park, PA 16802, USA
[5] Space Telescope Science Institute, 3700 San Martin Dr., Baltimore, MD 21218, USA
[6] Infrared Processing and Analysis Center, California Institute of Technology, Pasadena, CA 91125, USA
[7] NASA Ames Research Center, Moffett Field, CA 94035, USA
[8] Steward Observatory, University of Arizona, 933 North Cherry Avenue, Tucson, AZ 85721, USA
[9] Center for Astrophysics and Space Astronomy, University of Colorado, 389 UCB, Boulder, CO 80309, USA
[10] Minnesota Institute for Astrophysics, School of Physics and Astronomy, 116 Church Street, S. E., University of Minnesota, Minneapolis, MN 55455, USA
[11] Department of Physics, Florida State University, 77 Chieftain Way, Tallahassee, FL, 32306, USA
[12] MIT-Kavli Institute for Astrophysics and Space Research, 70 Vassar Street, Cambridge, MA 02139, USA
Received 2016 September 14; revised 2017 February 14; accepted 2017 February 18; published 2017 March 15

Abstract

SPitzer InfraRed Intensive Transients Survey—SPIRITS—is an ongoing survey of nearby galaxies searching for infrared (IR) transients with *Spitzer*/IRAC. We present the discovery and follow-up observations of one of our most luminous ($M_{[4.5]} = -17.1 \pm 0.4$ mag, Vega) and reddest ($[3.6]-[4.5] = 3.0 \pm 0.2$ mag) transients, SPIRITS 15c. The transient was detected in a dusty spiral arm of IC 2163 ($D \approx 35.5$ Mpc). Pre-discovery ground-based imaging revealed an associated, shorter-duration transient in the optical and near-IR (NIR). NIR spectroscopy showed a broad ($\approx$8400 km s^{-1}), double-peaked emission line of He I at 1.083 μm, indicating an explosive origin. The NIR spectrum of SPIRITS 15c is similar to that of the Type IIb SN 2011dh at a phase of $\approx$200 days. Assuming an $A_V = 2.2$ mag of extinction in SPIRITS 15c provides a good match between their optical light curves. The NIR light curves, however, show some minor discrepancies when compared with SN 2011dh, and the extreme [3.6]–[4.5] color has not been previously observed for any SN IIb. Another luminous ($M_{4.5} = -16.1 \pm 0.4$ mag) event, SPIRITS 14buu, was serendipitously discovered in the same galaxy. The source displays an optical plateau lasting $\gtrsim$80 days, and we suggest a scenario similar to the low-luminosity Type IIP SN 2005cs obscured by $A_V \approx 1.5$ mag. Other classes of IR-luminous transients can likely be ruled out in both cases. If both events are indeed SNe, this may suggest that $\gtrsim$18% of nearby core-collapse SNe are missed by currently operating optical surveys.

Key words: supernovae: general – supernovae: individual (SPIRITS 15c, SPIRITS 14buu) – surveys

1. Introduction

In the last few decades, the study of astrophysical transients has been revolutionized by the introduction of all-sky, high-cadence surveys dedicated to their discovery. The largest advances have been made in the optical, where the majority of time-domain surveys operate; the dynamic infrared (IR) sky is only now beginning to be explored. IR follow-up of optically discovered transients has revealed new classes of events that can be dominated by IR emission, especially at late times. At least two known classes of transients, with peak luminosities between those typical of novae and SNe, can develop IR-dominated spectral energy distributions (SEDs) as they evolve: (1) stellar mergers, or luminous red novae, e.g., M31-RV (Bond 2011, and references therein), V1309 Sco (Tylenda et al. 2011), V838 Mon (Bond et al. 2003; Sparks et al. 2008), the 2011 transient in NGC 4490 (hereafter NGC 4490-OT, Smith et al. 2016) and M101 OT2015-1 (M101-OT, Blagorodnova et al. 2017), SN 2008S-like events, or intermediate luminosity red transients (Prieto et al. 2008; Thompson et al. 2009; Kochanek 2011), also including NGC 300 OT2008-1 (hereafter NGC 300-OT, Bond et al. 2009; Humphreys et al. 2011) and PTF 10fqs (Kasliwal et al. 2011). Furthermore, otherwise luminous optical sources such as SNe may suffer extinction from obscuring dust, lending themselves to discovery and follow-up at IR wavebands where the effect of dust extinction is significantly reduced.

Previous searches for obscured SNe have thus been motivated by the notion that, if a significant fraction of SNe are heavily obscured, measurements of the SN rate from optical searches will only be lower limits (e.g., Grossan et al. 1999; Mattila & Meikle 2001; Maiolino et al. 2002; Cresci et al. 2007). Searches at near-IR (NIR) wavelengths have focused on the dense, highly star-forming, nuclear regions of starburst galaxies, luminous IR galaxies (LIRGS), and ultra-luminous IR galaxies (e.g., van Buren et al. 1994; Grossan et al. 1999; Maiolino et al. 2002; Mattila et al. 2002, 2004, 2005a, 2005b; Mannucci et al. 2003; Miluzio et al. 2013; Fox & Casper 2015). Multi-wavelength studies of two obscured SNe, SN 2010O and SN 2010 P, in LIRG Arp 299, for example, suggested its two merging components may have different extinction laws (Kankare et al. 2014; Romero-Cañizales et al. 2014). These searches have

[13] NSF Graduate Fellow.

uncovered a handful of additional obscured SNe, but have been limited by insufficient angular resolution to probe the densest regions of starburst galaxies.

High angular resolution studies using space-based telescopes or adaptive optics have found several candidates, and confirmed four obscured SNe (Cresci et al. 2007; Mattila et al. 2007; Kankare et al. 2008, 2012). The SN rate estimates from such searches are still a factor of 3–10 lower than is expected from the high star formation rates inferred from the far-IR luminosities of the surveyed galaxies (e.g., Cresci et al. 2007). Radio very long baseline interferometry studies of the innermost regions of LIRGs have, in fact, revealed scores of radio SNe and supernova (SN) remnants that have remained hidden at other wavelengths (Lonsdale et al. 2006; Pérez-Torres et al. 2009; Ulvestad 2009; Bondi et al. 2012; Herrero-Illana et al. 2012; Romero-Cañizales et al. 2012). A few bona fide radio transients have also been identified as obscured SNe II, e.g., an SN in the starburst Galaxy Mrk 297 (Yin & Heeschen 1991), VLA 121550.2+130654 (Gal-Yam et al. 2006), and SN 2008iz in M82 ($A_V > 10$ mag; Brunthaler et al. 2009, 2010; Mattila et al. 2013).

Even in "normal" star-forming galaxies in the nearby universe, where extinction is much less extreme, it has been suggested that the measured rates of core-collapse SNe (CCSNe) are still low compared to those expected from star-formation rates (Horiuchi et al. 2011). This indicates that optical surveys may be missing populations of nearby SNe that are either intrinsically faint or hidden by dust. By comparing the observed distribution of host extinctions for 13 SNe discovered within 12 Mpc between 2000 and 2011 to that predicted for smooth dust distributions in local galaxies, Mattila et al. (2012) estimate that 19^{+19}_{-10}% of local CCSNe are missed by rest-frame optical surveys in normal galaxies. Moderate levels of visual extinction ($A_V \sim$ few mag) in the less extreme star-forming environments of nearby galaxies are sufficient to dim some SNe beyond the detection limits of current optical surveys, further motivating IR transient searches of such hosts.

Since 2013 December, we have been conducting a systematic search for transients in the IR with the SPitzer InfraRed Intensive Transients Survey (SPIRITS; PID11063; PI M. Kasliwal). This is an ongoing, three-year targeted survey of 194 galaxies within 20 Mpc using the InfraRed Array Camera (IRAC; Fazio et al. 2004) aboard the *Spitzer Space Telescope* (*Spitzer*; Werner et al. 2004; Gehrz et al. 2007) at 3.6 and 4.5 μm ([3.6] and [4.5], respectively). Every galaxy in our sample has archival *Spitzer*/IRAC imaging, such that our observing cadence covers time baselines from one week to several years. In our first year, SPIRITS discovered over 1958 IR variable stars, and 43 transients. Four of these transients were in the luminosity range consistent with classical novae, and 21 were known SNe (for details, see Fox et al. 2016, Tinyanont et al. 2016, and Johansson et al. 2017). Fourteen were in the IR luminosity gap between novae and SNe and had no optical counterparts, possibly constituting a newly discovered class of IR-dominated transients (Kasliwal et al. 2017, submitted to ApJ).

Here, we report the discovery of two transients discovered in dusty spiral arms of the Galaxy IC 2163: SPIRITS 15c and SPIRITS 14buu. The IR luminosity of SPIRITS 15c was brighter than −17 mag, one of the most luminous transients discovered by SPIRITS to date and more luminous than the new classes of IR-dominated transients described above. Additionally, the spectrum of SPIRITS 15c is dominated by a broad emission line of He I, suggesting that this is an explosive event, such as an SN, but with significant dust extinction that obscured the transient in the optical. In Section 2, we describe the discovery and optical/IR follow-up observations of SPIRITS 15c, and the subsequent post-outburst, serendipitous discovery of SPIRITS 14buu. In Section 3, we describe the analysis of our photometric and spectroscopic data. In Section 4, we explore the possibility that SPIRITS 15c is an obscured SN based on the similarity of its NIR spectrum to that of the well-studied Type IIb SN 2011dh. Using a similar analysis, we consider that SPIRITS 14buu is yet another obscured SN, likely of Type IIP. We also consider non-supernova IR transient scenarios in Section 4.3, including stellar mergers, SN 2008S-like events, and the proposed helium nova V445 Pup. Finally, in Section 5, we summarize the observational characteristics of SPIRITS 15c and SPIRITS 14buu and present our conclusions.

2. SPIRITS Discovery and Follow-up Observations

We present the discoveries of SPIRITS 15c and SPIRITS 14buu, and describe observations of this event from our concomitant ground-based survey of SPIRITS galaxies.

2.1. Spitzer/IRAC Discovery in IC 2163

As part of the regular SPIRITS observing program, the interacting pair of late-type galaxies IC 2163 and NGC 2207 were observed at 10 epochs between 2014 January 13.9 and 2016 January 12.1. Image subtraction was performed using archival *Spitzer*/IRAC images from 2005 February 22.7 as references. For details on our image subtraction pipeline, see Kasliwal et al. (2017). On 2015 February 19, a transient source, designated SPIRITS 15c, was identified by the SPIRITS team in an image at [4.5] taken on 2015 February 4.4.[14] The [4.5] discovery image is shown in Figure 1.

SPIRITS 15c was discovered at a right ascension and declination of $06^h16^m28^s.49$, $-21°22'42''.2$ (J2000), coincident with a spiral arm of the galaxy IC 2163. We assume a distance modulus to IC 2163 of $\mu = 32.75 \pm 0.4$ mag from the mean of the *JHK* Tully–Fisher relation distance estimates (≈35.5 Mpc, Theureau et al. 2007 from NED[15]). IC 2163 has a redshift of $z = 0.00922$ ($v = 2765$ km s^{-1}, Elmegreen et al. 2000). We note that IC 2163 was originally selected as part of the SPIRITS sample based on an incorrect distance estimate that placed it within the 20 Mpc cutoff for SPIRITS galaxies. The foreground Galactic extinction toward IC 2163 is $A_V = 0.238$ mag from NED (Fitzpatrick 1999; Schlafly & Finkbeiner 2011). There is most likely additional extinction from the foreground spiral arm of NGC 2207.

Photometry was performed at the position of SPIRITS 15c on the reference subtracted images, using a 4-mosaicked-pixel aperture and a background annulus from 4–12 pixels. The extracted flux was multiplied by aperture corrections of 1.215

[14] The lag between the observations and discovery of SPIRITS 15c was due to the time for *Spitzer*/IRAC observations to be made available on the *Spitzer* Heritage Archive. Since 2015 May, the SPIRITS team has made extensive use of the *Spitzer* Early Release Data Program, allowing us to discovery transients within a few days of observation.

[15] The NASA/IPAC Extragalactic Database (NED) is operated by the Jet Propulsion Laboratory, California Institute of Technology, under contract with the National Aeronautics and Space Administration.

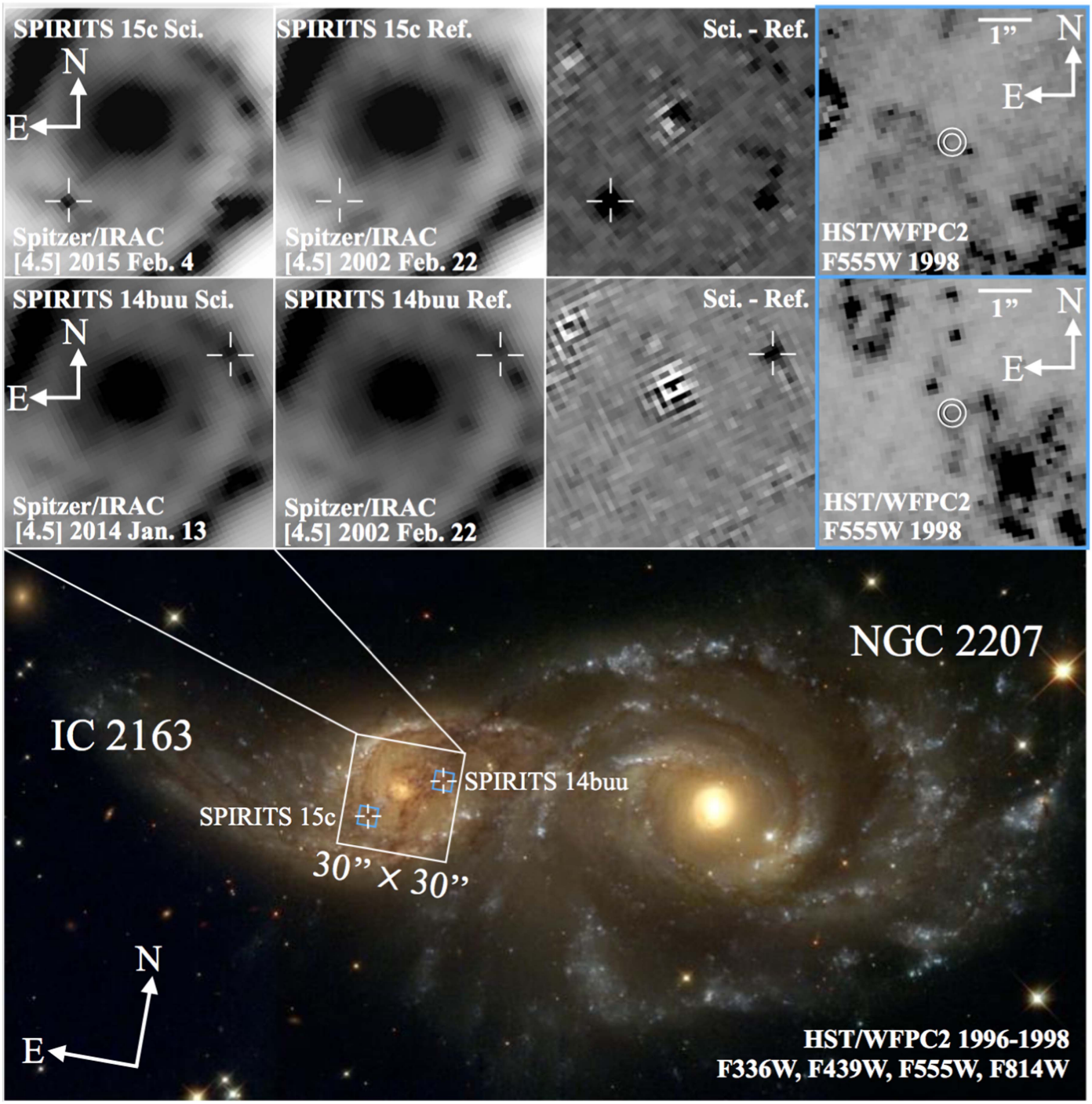

Figure 1. Bottom panel shows color-composite, archival *HST*/WFPC2 imaging of the interacting galaxy pair of IC 2163 and NGC 2207 from 1996-1998 in four filters (F336W and F439W in blue, F555W in green, and F814W in red). The image comes from the Hubble Heritage Project with credit to NASA and the Hubble Heritage Team (STScI/AURA). The approximate positions of SPIRITS 15c and SPIRITS 14buu in dusty spiral arms of IC 2163 are indicated with the crosshairs. The right panels of the top and middle rows show zoom-ins of the F555W image to the regions indicated by the blue squares for SPIRITS 15c and SPIRITS 14buu, respectively. The white circles show the 3- and 5-σ uncertainties on the precise positions of the transients. We are unable to identify an individual star as a candidate progenitor in either case. The left three panels in the top and middle rows show the $30'' \times 30''$ region indicated by the white zoom-in box. The first row of panels from the left are the *Spitzer*/IRAC discovery science frames at [4.5] from 2015 February 4.4 (top row; SPIRITS 15c) and 2014 January 13.9 (middle row; SPIRITS 14buu), the second row are the reference images from 2005 February 22.7 (PID3544; PI D. M. Elmegreen), and the third row are the science—reference subtraction images, clearly showing the new, transient sources. We note that, in the SPIRITS 15c discovery and subtraction images, the apparent variability of the galaxy nucleus is likely a subtraction artifact, as both positive and negative flux appear in the subtracted frame. The apparent new source directly to the west of SPIRITS 15c, which is not present at [3.6] or at any other epoch, is also likely spurious, given its boxy and irregular shape.

and 1.233 for [3.6] and [4.5], respectively, as outlined in the IRAC instrument handbook. The photometric measurements, given in Table 1, indicate a high luminosity of $M_{[4.5]} = -17.1 \pm 0.4$ mag at the distance of IC 2163 and an extremely red color of [3.6]–[4.5] $= 3.0 \pm 0.2$ mag at the epoch of discovery. SPIRITS 15c was not detected in earlier images taken on 2014 June 8.7 to a limiting magnitude of $m \gtrsim 18.3$ mag at [4.5] (-14.5 mag absolute), providing an age constraint for

Table 1
Photometry of SPIRITS 15c

UT Date	MJD	Phase[a] (days)	Tel./Inst.	Band	Apparent Magnitude[b,c] (mag)	Absolute Magnitude[c,d] (mag)
2013 Dec 16.1	56642.1	−248	NOTCam	K_s	>17.0	>−15.8
2013 Dec 24.3	56650.3	−240	P60	g	>20.4	>−12.7
2014 Jan 13.9	56670.9	−220	*Spitzer*/IRAC	[3.6]	>18.6	>−14.2
2014 Jan 13.9	56670.9	−220	*Spitzer*/IRAC	[4.5]	>18.4	>−14.3
2014 Jan 10.2	56667.2	−223	du Pont/RetroCam	Y	>19.7	>−13.2
2014 Jan 10.2	56667.2	−223	du Pont/RetroCam	J	>19.2	>−13.6
2014 Jan 10.2	56667.2	−223	du Pont/RetroCam	H	>18.8	>−14.0
2014 Feb 06.2	56694.2	−196	Baade/IMACS	WB6226−7171	>22.0	>−10.9
2014 Feb 18.2	56706.2	−184	Swope/CCD	g	>20.7	>−12.3
2014 Feb 18.2	56706.2	−184	Swope/CCD	r	>20.7	>−12.2
2014 Feb 18.2	56706.2	−184	Swope/CCD	i	>20.5	>−12.4
2014 Mar 07.1	56723.1	−167	Baade/FourStar	J	>20.4	>−12.5
2014 Mar 15.1	56731.1	−159	du Pont/RetroCam	Y	>20.7	>−12.2
2014 Mar 15.1	56731.1	−159	du Pont/RetroCam	J	>20.4	>−12.4
2014 Mar 16.1	56732.1	−158	du Pont/RetroCam	H	>19.0	>−13.8
2014 Apr 13.0	56760.0	−130	Swope/CCD	r	>20.6	>−12.3
2014 Apr 13.0	56760.0	−130	Swope/CCD	i	>20.5	>−12.4
2014 May 13.7	56790.7	−100	*Spitzer*/IRAC	[3.6]	>18.8	>−14.0
2014 May 13.7	56790.7	−100	*Spitzer*/IRAC	[4.5]	>18.6	>−14.2
2014 May 27.9	56804.9	−86	LCOGT-1 m/CCD	i	>18.7	>−14.2
2014 Jun 08.7	56816.7	−74	*Spitzer*/IRAC	[3.6]	>18.7	>−14.0
2014 Jun 08.7	56816.7	−74	*Spitzer*/IRAC	[4.5]	>18.3	>−14.4
2014 Jul 25.4	56863.4	−27	LCOGT-1 m/CCD	i	>19.0	>−13.9
2014 Aug 21.4	56890.4	0	LCOGT-1 m/CCD	i	17.66 (0.06)	−15.2
2014 Sep 20.3	56920.3	30	LCOGT-1 m/CCD	i	18.25 (0.06)	−14.6
2014 Sep 29.0	56929.0	39	Swope/CCD	g	20.9 (0.2)	−12.1
2014 Sep 29.0	56929.0	39	Swope/CCD	r	19.2 (0.1)	−13.7
2014 Sep 29.0	56929.0	39	Swope/CCD	i	18.57 (0.09)	−14.3
2014 Oct 23.3	56953.3	63	LCOGT-1 m/CCD	r	19.6 (0.3)	−13.3
2014 Oct 23.3	56953.3	63	LCOGT-1 m/CCD	i	19.1 (0.3)	−13.8
2014 Nov 15.2	56976.2	86	LCOGT-1 m/CCD	r	20.4 (0.3)	−12.6
2014 Nov 15.2	56976.2	86	LCOGT-1 m/CCD	i	19.5 (0.3)	−13.4
2014 Nov 20.4	56981.4	91	Lemmon-1.5 m/2MASSCam	J	>14.3	>−18.5
2014 Nov 20.4	56981.4	91	Lemmon-1.5 m/2MASSCam	H	>13.5	>−19.3
2014 Nov 20.4	56981.4	91	Lemmon-1.5 m/2MASSCam	K_s	>13.1	>−19.7
2014 Dec 05.3	56996.3	106	du Pont/RetroCam	Y	18.8 (0.2)	−14.1
2014 Dec 05.3	56996.3	106	du Pont/RetroCam	H	17.79 (0.08)	−15.0
2014 Dec 14.3	57005.3	115	LCOGT-1 m/CCD	r	>19.6	>−13.3
2014 Dec 14.3	57005.3	115	LCOGT-1 m/CCD	i	>19.2	>−13.7
2014 Dec 20.2	57011.2	121	Swope/CCD	g	>21.1	>−11.9
2014 Dec 20.2	57011.2	121	Swope/CCD	r	>20.8	>−12.1
2014 Dec 20.2	57011.2	121	Swope/CCD	i	>20.4	>−12.5
2015 Jan 13.2	57035.2	145	LCOGT-1 m/CCD	r	>19.6	>−13.3
2015 Jan 13.2	57035.2	145	LCOGT-1 m/CCD	i	>19.2	>−13.7
2015 Jan 16.3	57038.3	148	Lemmon-1.5 m/2MASSCam	J	>13.5	>−19.3
2015 Jan 16.3	57038.3	148	Lemmon-1.5 m/2MASSCam	H	>12.7	>−20.1
2015 Jan 16.3	57038.3	148	Lemmon-1.5 m/2MASSCam	K_s	>12.6	>−20.2
2015 Jan 20.0	57042.0	152	Baade/IMACS	WB6226 − 7171	21.4 (0.1)	−11.5
2015 Jan 29.1	57051.1	161	du Pont/RetroCam	Y	19.9 (0.2)	−12.9
2015 Jan 29.1	57051.1	161	du Pont/RetroCam	J	19.8 (0.1)	−13.0
2015 Jan 29.1	57051.1	161	du Pont/RetroCam	H	18.8 (0.1)	−14.0
2015 Feb 02.2	57055.2	165	Swope/CCD	g	>20.2	>−12.8
2015 Feb 02.2	57055.2	165	Swope/CCD	r	>20.1	>−12.8
2015 Feb 02.2	57055.2	165	Swope/CCD	i	>20.1	>−12.8
2015 Feb 04.4	57057.4	167	*Spitzer*/IRAC	[3.6]	18.7 (0.2)	−14.1
2015 Feb 04.4	57057.4	167	*Spitzer*/IRAC	[4.5]	15.68 (0.02)	−17.1
2015 Feb 13.0	57066.0	176	LCOGT-1 m/CCD	r	>19.0	>−13.9
2015 Feb 13.0	57066.0	176	LCOGT-1 m/CCD	i	>18.9	>−14.0
2015 Feb 18.0	57071.0	181	Baade/FourStar	K_s	19.17 (0.08)	−13.6
2015 Feb 20.2	57073.2	183	Lemmon-1.5 m/2MASSCam	J	>14.3	>−18.5
2015 Feb 20.2	57073.2	183	Lemmon-1.5 m/2MASSCam	H	>13.5	>−19.3

Table 1
(Continued)

UT Date	MJD	Phase[a] (days)	Tel./Inst.	Band	Apparent Magnitude[b,c] (mag)	Absolute Magnitude[c,d] (mag)
2015 Feb 20.2	57073.2	183	Lemmon-1.5 m/2MASSCam	K_s	>13.2	>−19.6
2015 Mar 09.1	57090.1	200	du Pont/RetroCam	Y	>20.3	>−12.6
2015 Mar 09.1	57090.1	200	du Pont/RetroCam	J	>19.6	>−13.2
2015 Mar 09.1	57090.1	200	du Pont/RetroCam	H	>18.8	>−14.0
2015 Mar 13.1	57094.1	204	Swope/CCD	g	>20.6	>−12.4
2015 Mar 13.1	57094.1	204	Swope/CCD	r	>19.9	>−13.0
2015 Mar 13.1	57094.1	204	Swope/CCD	i	>19.5	>−13.4
2015 Mar 14.0	57095.0	205	du Pont/RetroCam	Y	>20.2	>−12.6
2015 Mar 14.0	57095.0	205	du Pont/RetroCam	J	>20.3	>−12.5
2015 Mar 14.0	57095.0	205	du Pont/RetroCam	H	>19.4	>−13.4
2015 Mar 15.0	57096.0	206	LCOGT-1 m/CCD	r	>19.2	>−13.7
2015 Mar 15.0	57096.0	206	LCOGT-1 m/CCD	i	>18.8	>−14.1
2015 Mar 15.0	57096.0	206	Kuiper/Mont4k	R	>20.5	>−12.4
2015 Apr 05.1	57117.1	227	du Pont/RetroCam	Y	>20.2	>−12.7
2015 Apr 05.1	57117.1	227	du Pont/RetroCam	J	>19.3	>−13.5
2015 Apr 05.1	57117.1	227	du Pont/RetroCam	H	>18.5	>−14.3
2015 Apr 16.4	57128.4	238	LCOGT-1 m/CCD	r	>20.1	>−12.8
2015 Apr 16.4	57128.4	238	LCOGT-1 m/CCD	i	>19.5	>−13.4
2015 Apr 30.0	57142.0	252	du Pont/RetroCam	Y	>20.6	>−12.3
2015 Apr 30.0	57142.0	252	du Pont/RetroCam	J	>20.1	>−12.7
2015 Apr 30.0	57142.0	252	du Pont/RetroCam	H	>18.9	>−13.8
2015 May 26.9	57168.9	278	*Spitzer*/IRAC	[3.6]	>18.8	>−14.0
2015 May 26.9	57168.9	278	*Spitzer*/IRAC	[4.5]	17.01 (0.06)	−15.7
2015 Jun 03.8	57176.8	286	*Spitzer*/IRAC	[3.6]	>18.9	>−13.9
2015 Jun 03.8	57176.8	286	*Spitzer*/IRAC	[4.5]	17.05 (0.07)	−15.7
2015 Jun 24.1	57197.1	307	*Spitzer*/IRAC	[3.6]	>18.7	>−14.1
2015 Jun 24.1	57197.1	307	*Spitzer*/IRAC	[4.5]	17.32 (0.08)	−15.4
2015 Sep 05.4	57270.4	380	Baade/FourStar	J	>20.2	>−12.6
2015 Sep 05.4	57270.4	380	Baade/FourStar	H	>19.9	>−12.9
2015 Sep 05.4	57270.4	380	Baade/FourStar	K_s	>19.5	>−13.3
2015 Nov 19.3	57345.3	455	du Pont/RetroCam	Y	>20.9	>−11.9
2015 Nov 19.3	57345.3	455	du Pont/RetroCam	J	>20.7	>−12.1
2015 Nov 19.3	57345.3	455	du Pont/RetroCam	H	>19.8	>−13.0
2015 Nov 22.3	57348.3	458	du Pont/RetroCam	Y	>20.7	>−12.2
2015 Nov 22.3	57348.3	458	du Pont/RetroCam	J	>20.1	>−12.7
2015 Nov 22.3	57348.3	458	du Pont/RetroCam	H	>19.5	>−13.3
2015 Dec 23.0	57379.0	489	*Spitzer*/IRAC	[3.6]	>18.8	>−14.0
2015 Dec 23.0	57379.0	489	*Spitzer*/IRAC	[4.5]	>18.5	>−14.3
2015 Dec 30.1	57386.1	496	*Spitzer*/IRAC	[3.6]	>18.7	>−14.0
2015 Dec 30.1	57386.1	496	*Spitzer*/IRAC	[4.5]	>18.4	>−14.3
2016 Jan 12.1	57399.1	509	*Spitzer*/IRAC	[3.6]	>18.8	>−14.0
2016 Jan 12.1	57399.1	509	*Spitzer*/IRAC	[4.5]	>18.3	>−14.4

Notes.
[a] Phase is number of days since the earliest detection of this event on 2014 August 21.4 (MJD = 56890.4).
[b] 1-σ uncertainties are given in parentheses.
[c] 5-σ limiting magnitudes are given for non-detections.
[d] Absolute magnitudes corrected for galactic extinction for IC 2163 from NED.

SPIRITS 15c as an active mid-IR (MIR) source of 240.7 days. Additional detections were made at [4.5] in SPIRITS observations of IC 2163 on 2015 May 26.9, June 3.8, and June 24.1, fading by ≈2 mag in 140 days. On 2015 December 23.0, SPIRITS 15c was undetected at [4.5] and remained so in all subsequent SPIRITS observations through the most recent one on 2016 January 12.1. The source was undetected at [3.6] in all post-discovery epochs of *Spitzer*/IRAC observation. The 5-σ depth in the reference images at the position of SPIRITS 15c is 14.9 mag (≈−17.9 mag absolute) in both bands, and thus, we are unable to place meaningful constraints on the IR properties of the progenitor system. The full sequence of photometric measurements from *Spitzer*/IRAC for SPIRITS 15c is summarized in Table 1 and shown in Figure 2, along with the NIR and optical measurements described below in Section 2.2.

2.1.1. Host Galaxy Properties

Elmegreen et al. (2016) report global values of the 24 μm flux density from a *Spitzer*/MIPS 2013 archival image of

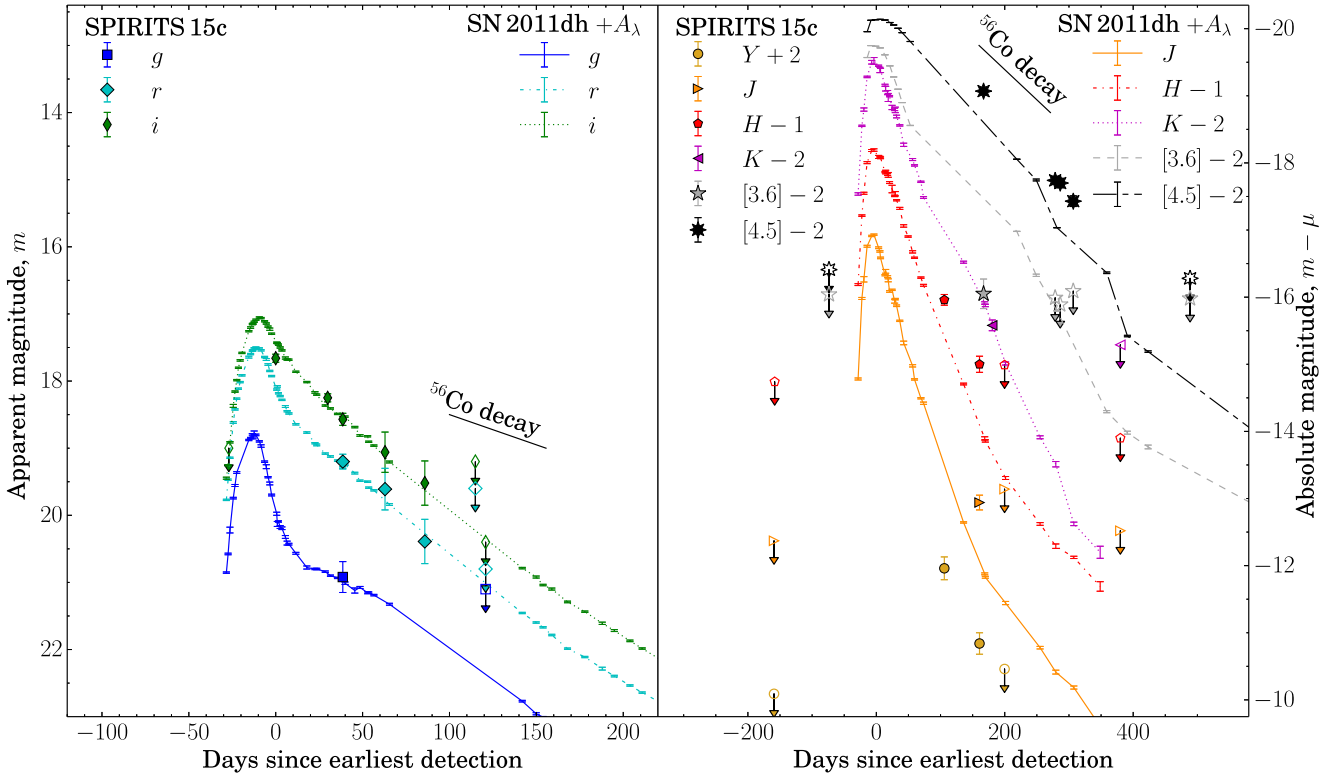

Figure 2. Optical (*gri*; AB magnitudes; left panel), and IR (*YJHK*$_s$, [3.6], and [4.5]; Vega magnitudes; right panel) light curves of SPIRITS 15c (points) and the Type IIb SN 2011dh (lines). Unfilled points with downward arrows indicate upper limits. Error bars are shown, but are sometimes smaller than the points. Time on the *x*-axis is given as the number of days since the earliest detection of SPIRITS 15c on 2014 August 21.4 (MJD = 56890.4). The light curves of SN 2011dh are shifted in apparent magnitude to the distance of SPIRITS 15c, with applied total reddening characterized by $E(B-V)_{\rm MW}+E(B-V)_{\rm host}=0.72$ mag, or $A_V\approx 2.2$ mag of extinction assuming a standard $R_V=3.1$ extinction law (Fitzpatrick 1999; Chapman et al. 2009; Schlafly & Finkbeiner 2011). The phase of the SN 2011dh light curves is set so that the earliest detection of SN 2011dh coincides with the most constraining non-detection preceding the outburst of SPIRITS 15c. For comparison, we also show the expected decay rate for a light curve powered by the radioactive decay of ^{56}Co (see Gehrz 1988; Gehrz & Ney 1990).

$S_\nu(24\ \mu{\rm m})=5.9\times10^2$ mJy for IC 2136, and 2.06×10^4 mJy for the galaxy pair as a whole. They also give global Hα fluxes, derived from narrowband Hα and broadband *R* images from Elmegreen et al. (2001), of $S({\rm H}\alpha)=5.9\times10^{-13}$ and 3.49×10^{-12} erg s^{-1} cm^{-2} for IC 2163 and the pair as a whole, respectively. Combining these, and following Kennicutt et al. (2009), gives global star-formation rates of 1.9 $M_\odot$ yr^{-1} for IC 2163 and 6.8 $M_\odot$ yr^{-1} for both galaxies combined. The rate of SNe associated with this galaxy pair is also high, with five known SNe hosted in IC 2163 and NGC 2207 since 1975. These include four CCSNe (SN 1999ec, Jha et al. 1999; Modjaz & Li 1999; SN 2003 H, Filippenko et al. 2003; SN 2013ai, Conseil et al. 2013; SN 2010jp, Smith et al. 2012) and one thermonuclear SN (SN 1975 A, Kirshner et al. 1976). The most recent SN associated with the galaxy pair, SN 2010jp, is a peculiar SN IIn with evidence for strong interaction with a dense circumstellar medium (CSM) and a bipolar, jet-driven explosion (Smith et al. 2012).

In a 3.6 arcsec aperture centered on the location of SPIRITS 15c, $S_\nu(24\ \mu{\rm m})=8.38$ mJy, as measured in the HiRes devconvolution image from Velusamy et al. (2008) (1.9 arcsec resolution). In the same aperture, $S({\rm H}\alpha)=1.25\times10^{-14}$ erg s^{-1} cm^{-2}. Additionally, the ^{12}CO(1-0) (115.27 GHz, 2.6 mm) line flux in this region, measured with ALMA, implies a mean line-of-sight H_2 surface density of $\Sigma_{\rm H_2}=13.7\ M_\odot$ pc^{-2} (Elmegreen et al. 2016; Kaufman et al. 2016, private communication). Estimates of the star-formation rate, using Hα as tracer in such a small aperture, will include stochastic effects related to including too few O stars, but these measurements suggest ongoing star formation in the vicinity of SPIRITS 15c, and that the transient may be associated with a young stellar population. The heliocentric radial velocity in the ALMA CO velocity image at the nearest non-blanked pixel to SPIRITS 15c is $v_{\rm CO,helio}=2827$ km s^{-1} (2″ separation; Elmegreen et al. 2016; Kaufman et al. 2016, private communication). We adopt this value as the velocity of SPIRITS 15c with respect to the observer frame throughout this paper.

2.2. Ground-based Imaging

To supplement our *Spitzer*/IRAC observations, the SPIRITS team is undertaking a concomitant, ground-based survey of SPIRITS galaxies in the optical and NIR, using a number of telescopes and instruments.

IC 2163 was imaged at several epochs in *gri* with the CCD camera on the Swope Telescope at Las Campanas Observatory (LCO). NIR *YJH* imaging of SPIRITS 15c was also obtained at several epochs with the RetroCam IR camera on the du Pont Telescope, and *J*, *H*, and K_s-band images were obtained with the FourStar IR camera on the *Magellan* Baade Telescope at LCO (Persson et al. 2013). Photometry was extracted using simple aperture photometry, with the aperture size defined by the seeing in each image, and calibrated against SDSS field stars for the optical images and 2MASS stars for the NIR images. For *Y*-band images, we adopt the conversion from 2MASS used for the Wide Field Camera on the United

Kingdom Infrared Telescope from Hodgkin et al. (2009). Image subtraction was performed for the Swope/CCD and du Pont/Retrocam images using template images taken on 2015 March 13.2 (after SPIRITS 15c had faded) and 2014 January 10.2, respectively, to obtain more accurate photometry and deeper limits from non-detection images.

We also obtained optical imaging with the Las Cumbres Observatory Global Telescope (LCOGT; Brown et al. 2013) Network 1 m telescopes in the *r*- and *i*-bands. Photometry was performed by simultaneously fitting the point-spread function of the transient, measured using SDSS field stars, and background, modeled using low-order polynomials. The photometric measurements were also calibrated against SDSS field stars.

Additional imaging of IC 2163 was obtained on 2014 February 6.2 and 2015 January 20.0 with the Inamori *Magellan* Areal Camera and Spectrograph (IMACS) on the *Magellan* Baade Telescope, using a wide-band, red filter (WB6226-7171 calibrated to SDSS r'); on 2015 March 16, using the Mont4k on the Kuiper 61″ Telescope in *R*-band; on 2013 December 24.3, with the optical camera on the 60-in telescope at Palomar observatory (P60) in *g*, *r*, and *i*; and on 2013 December 16.1 in K_s-band, with the Nordic Optical Telescope near-infrared Camera and spectrograph (NOTCam), at the Observatorio del Roque de los Muchachos.

The earliest detection of SPIRITS 15c on 2014 August 21.4 (MJD = 56890.4) was also the observed optical peak at $i = 17.66 \pm 0.06$ mag. Correcting for galactic extinction gives a peak absolute magnitude $M_i \leqslant -15.1 \pm 0.4$ mag, where any additional foreground or host extinction would imply a higher intrinsic luminosity. Throughout the rest of this paper, we refer to days t since the earliest detection of SPIRITS 15c on this date. Our most stringent constraint on the age of SPIRITS 15c is the 28.4-day window between the earliest detection and the previous optical non-detection on 2014 July 24.0. The observed optical colors at $t = 38.6$ days were quite red with $g-r = 1.71 \pm 0.15$ mag and $g-i = 2.24 \pm 0.15$ mag. By $t = 120.8$ days, SPIRITS 15c had faded beyond detection with Swope/CCD, but was still detected in the Baade/IMACS image at 21.4 ± 0.1 mag.

At $t = 105.9$ days, SPIRITS 15c was detected in the NIR with $H = 17.84 \pm 0.06$ mag (-14.91 ± 0.4 mag absolute), and a red NIR color with $Y - H = 1.04 \pm 0.09$ mag. The transient then faded in the NIR by 1 mag at nearly constant color over the next 54.8 days. All of our photometric measurements for SPIRITS 15c are summarized in Table 1, and the light curves are shown in Figure 2.

2.3. Another Transient Discovery: SPIRITS 14buu

During the analysis of our imaging data, a second transient was serendipitously noticed in IC 2163 at a right ascension and declination of $06^{\rm h}16^{\rm m}27^{\rm s}.2$, $-21°22'29''.2$ (J2000), located in a spiral arm directly on the other side of the galaxy from SPIRITS 15c. This transient was active in January 2014 SPIRITS *Spitzer*/IRAC data, before the implementation of our automated image subtraction and candidate identification pipeline. It was retroactively assigned the name SPIRITS 14buu. We show the [4.5] discovery image in Figure 1.

The earliest detection of this event is in the P60 *r*- and *i*-band images taken on 2013 December 24.3 (MJD = 56650.3). It was not detected in the K_s NOTCam image on 2013 December 16.1 to $K_s > 16.6$ mag (>-16.2 mag absolute), but this limit is not deep enough to constrain the age of SPIRITS 14buu. The optical and IR light curves of SPIRITS 14buu are given in Table 2 and shown in Figure 3. In the *r*- and *i*-bands, the source displays a plateau lasting at least 80 days at $i = 19.2 \pm 0.1$ mag ($M_i = -13.7$ mag absolute) and with $r - i = 0.7 \pm 0.2$ mag. The source is undetected in *g*-band indicating $g - i \gtrsim 1.7$ mag. Following the plateau, the optical light curves fall off steeply, dropping in *i*-band by $\gtrsim$1.1 mag in $\lesssim$24 days. A luminous NIR counterpart was detected during the optical plateau with $H = 17.44 \pm 0.07$ ($M_H = -15.3$ absolute). The source shows red NIR colors with $Y - H = 0.76 \pm 0.09$ and $J - H = 0.4 \pm 0.1$ mag, and a slow decline in the NIR of $\approx$0.2 mag over 65 days.

SPIRITS 14buu was also detected as a luminous MIR source with *Spitzer*/IRAC. The observed MIR peak occurred at 17 days after the earliest detection of this event at 16.7 ± 0.1 mag (-16.1 absolute) in both bands. At [4.5], the light curve declines slowly by 0.6 ± 0.1 mag over 145.8 days, extending well past the time of the plateau fall-off in the optical. At [3.6], the source fades more quickly developing a red [3.6]–[4.5] color of 1.2 ± 0.2 mag by 166.4 days after the earliest detection. The source faded beyond detection in both bands by 407.1 days.

We further describe the characteristics of this transient and discuss possible physical interpretations below in Section 4.2.

2.4. Archival Hubble Space Telescope (HST) Imaging

Images of the interacting[16] galaxies IC 2163 and NGC 2207 were obtained with the *HST* on 1998 November 11 in program GO-6483 (PI: D. Elmegreen). These observations used the Wide Field Planetary Camera 2 (WFPC2), and fortuitously covered the site of SPIRITS 15c and SPIRITS 14buu, some 17 years before their outbursts. Images of this galaxy pair were also included in the Hubble Heritage collection. In the bottom panel of Figure 1, we show the color-composite Hubble Heritage Project[17] image of the field containing the transients made from imaging data in the F814W (red), F555W (green), F439W, and F336W (blue) filters. We note the locations of SPIRITS 15c and SPIRITS 14buu in dusty spiral arms of IC 2163.

In the *HST* images of IC 2163, the location of SPIRITS 15c unfortunately lies close to the edge of the PC chip, so we did not further analyze those frames. In the images of NGC 2207, the SPIRITS 15c site is well-placed in the WF2 field. We chose two sets of dithered frames taken with the F555W filter ($\sim V$; exposures of 3×160 s plus one of 180 s), and with F814W ($\sim I$; 4×180 s). We registered and combined these two sets of images, using standard tasks in IRAF.[18]

To find the precise location of SPIRITS 15c in the WFPC2 frames, we employed the Baade/IMACS WB6226-7171 image from 2015 January 20.0. Using centroid measurements for 15 stars detected both in the Baade/IMACS frame and in the two combined WFPC2 images, we determined the geometric

[16] Based on observations made with the NASA/ESA *Hubble Space Telescope*, obtained from the data archive at the Space Telescope Science Institute. STScI is operated by the Association of Universities for Research in Astronomy, Inc. under NASA contract NAS 5-26555.

[17] Image Credit: NASA and The Hubble Heritage Team (STScI/AURA).

[18] IRAF is distributed by the National Optical Astronomy Observatory, which is operated by the Association of Universities for Research in Astronomy (AURA) under a cooperative agreement with the National Science Foundation.

Table 2
Photometry of SPIRITS 14buu

UT Date	MJD	Phase[a] (days)	Tel./Inst.	Band	Apparent Magnitude[b,c] (mag)	Absolute Magnitude[c,d] (mag)
2013 Dec 16.1	56642.1	−8	NOTCam	K_s	>16.6	>−16.2
2013 Dec 24.3	56650.3	0	P60	g	>20.4	>−12.6
2013 Dec 24.3	56650.3	0	P60	r	20.0 (0.3)	−13.0
2013 Dec 24.3	56650.3	0	P60	i	19.4 (0.3)	−13.5
2014 Jan 10.2	56667.2	17	du Pont/RetroCam	Y	18.20 (0.06)	−14.6
2014 Jan 10.2	56667.2	17	du Pont/RetroCam	J	17.80 (0.08)	−15.0
2014 Jan 10.2	56667.2	17	du Pont/RetroCam	H	17.44 (0.07)	−15.3
2014 Jan 13.9	56670.9	21	*Spitzer*/IRAC	[3.6]	16.69 (0.08)	−16.1
2014 Jan 13.9	56670.9	21	*Spitzer*/IRAC	[4.5]	16.70 (0.05)	−16.1
2014 Feb 18.2	56706.2	56	Swope/CCD	g	>20.9	>−12.2
2014 Feb 18.2	56706.2	56	Swope/CCD	r	20.0 (0.2)	−12.9
2014 Feb 18.2	56706.2	56	Swope/CCD	i	19.2 (0.1)	−13.7
2014 Mar 07.1	56723.1	73	Baade/FourStar	J	18.09 (0.02)	−14.7
2014 Mar 14.0	56730.0	80	Swope/CCD	g	>20.8	>−12.2
2014 Mar 14.0	56730.0	80	Swope/CCD	r	20.0 (0.2)	−13.0
2014 Mar 14.0	56730.0	80	Swope/CCD	i	19.4 (0.1)	−13.5
2014 Mar 15.1	56731.1	81	du Pont/RetroCam	Y	18.43 (0.08)	−14.4
2014 Mar 15.1	56731.1	81	du Pont/RetroCam	J	18.11 (0.06)	−14.7
2014 Mar 16.1	56732.1	82	du Pont/RetroCam	H	17.6 (0.1)	−15.2
2014 Apr 13.0	56760.0	110	Swope/CCD	g	>20.8	>−12.2
2014 Apr 13.0	56760.0	110	Swope/CCD	r	>20.6	>−12.4
2014 Apr 13.0	56760.0	110	Swope/CCD	i	>20.5	>−12.4
2014 May 13.7	56790.7	140	*Spitzer*/IRAC	[3.6]	18.0 (0.2)	−14.8
2014 May 13.7	56790.7	140	*Spitzer*/IRAC	[4.5]	17.13 (0.06)	−15.6
2014 Jun 08.7	56816.7	166	*Spitzer*/IRAC	[3.6]	18.4 (0.2)	−14.3
2014 Jun 08.7	56816.7	166	*Spitzer*/IRAC	[4.5]	17.28 (0.08)	−15.5
2014 Sep 29.4	56929.4	279	Swope/CCD	g	>21.5	>−11.5
2014 Sep 29.4	56929.4	279	Swope/CCD	r	>21.0	>−11.9
2014 Sep 29.4	56929.4	279	Swope/CCD	i	>20.7	>−12.2
2014 Dec 05.3	56996.3	346	du Pont/RetroCam	Y	>20.5	>−12.3
2014 Dec 05.3	56996.3	346	du Pont/RetroCam	H	>20.1	>−12.7
2014 Dec 20.2	57011.2	361	Swope/CCD	g	>21.4	>−11.6
2014 Dec 20.2	57011.2	361	Swope/CCD	r	>21.0	>−11.9
2014 Dec 20.2	57011.2	361	Swope/CCD	i	>20.6	>−12.3
2015 Jan 29.1	57051.1	401	du Pont/RetroCam	Y	>21.2	>−11.6
2015 Jan 29.1	57051.1	401	du Pont/RetroCam	J	>20.6	>−12.2
2015 Jan 29.1	57051.1	401	du Pont/RetroCam	H	>20.2	>−12.6
2015 Feb 02.2	57055.2	405	Swope/CCD	g	>20.1	>−12.9
2015 Feb 02.2	57055.2	405	Swope/CCD	r	>20.1	>−12.8
2015 Feb 02.2	57055.2	405	Swope/CCD	i	>20.1	>−12.8
2015 Feb 04.4	57057.4	407	*Spitzer*/IRAC	[3.6]	>18.6	>−14.2
2015 Feb 04.4	57057.4	407	*Spitzer*/IRAC	[4.5]	>17.8	>−15.0
2015 Feb 18.0	57071.0	421	Baade/FourStar	K_s	>19.1	>−13.6
2015 Mar 09.1	57090.1	440	du Pont/RetroCam	Y	>20.2	>−12.6
2015 Mar 09.1	57090.1	440	du Pont/RetroCam	J	>19.7	>−13.1
2015 Mar 09.1	57090.1	440	du Pont/RetroCam	H	>19.2	>−13.6
2015 Mar 13.1	57094.1	444	Swope/CCD	g	>21.5	>−11.5
2015 Mar 13.1	57094.1	444	Swope/CCD	r	>21.0	>−12.0
2015 Mar 13.1	57094.1	444	Swope/CCD	i	>20.4	>−12.5
2015 Mar 14.0	57095.0	445	du Pont/RetroCam	J	>19.9	>−12.9
2015 Apr 05.1	57117.1	467	du Pont/RetroCam	Y	>20.0	>−12.8
2015 Apr 05.1	57117.1	467	du Pont/RetroCam	J	>19.4	>−13.5
2015 Apr 05.1	57117.1	467	du Pont/RetroCam	H	>18.9	>−13.9
2015 Apr 30.0	57142.0	492	du Pont/RetroCam	Y	>20.6	>−12.2
2015 Apr 30.0	57142.0	492	du Pont/RetroCam	J	>20.1	>−12.7
2015 Apr 30.0	57142.0	492	du Pont/RetroCam	H	>19.3	>−13.5
2015 May 26.9	57168.9	519	*Spitzer*/IRAC	[3.6]	>18.8	>−14.0
2015 May 26.9	57168.9	519	*Spitzer*/IRAC	[4.5]	>17.7	>−15.0
2015 Jun 03.8	57176.8	526	*Spitzer*/IRAC	[3.6]	>18.7	>−14.1
2015 Jun 03.8	57176.8	526	*Spitzer*/IRAC	[4.5]	>17.6	>−15.1
2015 Jun 24.1	57197.1	547	*Spitzer*/IRAC	[3.6]	>18.4	>−14.3

Table 2
(Continued)

UT Date	MJD	Phase[a] (days)	Tel./Inst.	Band	Apparent Magnitude[b,c] (mag)	Absolute Magnitude[c,d] (mag)
2015 Jun 24.1	57197.1	547	*Spitzer*/IRAC	[4.5]	>17.7	>−15.1
2015 Sep 05.4	57270.4	620	Baade/FourStar	*J*	>19.6	>−13.2
2015 Sep 05.4	57270.4	620	Baade/FourStar	*H*	>19.4	>−13.4
2015 Sep 05.4	57270.4	620	Baade/FourStar	K_s	>19.0	>−13.8
2015 Nov 22.3	57348.3	698	du Pont/RetroCam	*Y*	>20.8	>−12.0
2015 Nov 22.3	57348.3	698	du Pont/RetroCam	*H*	>20.0	>−12.8
2015 Dec 23.0	57379.0	729	*Spitzer*/IRAC	[3.6]	>18.5	>−14.3
2015 Dec 23.0	57379.0	729	*Spitzer*/IRAC	[4.5]	>17.6	>−15.1
2015 Dec 30.1	57386.1	736	*Spitzer*/IRAC	[3.6]	>18.4	>−14.4
2015 Dec 30.1	57386.1	736	*Spitzer*/IRAC	[4.5]	>17.8	>−15.0
2016 Jan 12.1	57399.1	749	*Spitzer*/IRAC	[3.6]	>18.3	>−14.5
2016 Jan 12.1	57399.1	749	*Spitzer*/IRAC	[4.5]	>17.7	>−15.1
2016 Mar 02.1	57449.1	799	du Pont/RetroCam	*Y*	>20.4	>−12.5
2016 Mar 02.1	57449.1	799	du Pont/RetroCam	*H*	>18.5	>−14.2

Notes.
[a] Phase is number of days since the earliest detection of this event on 2014 August 21.4 (MJD = 56650.3).
[b] 1-σ uncertainties are given in parentheses.
[c] 5-σ limiting magnitudes are given for non-detections.
[d] Absolute magnitudes corrected for Galactic extinction for IC 2163 from NED.

transformation from *Magellan* to WFPC2 using the STSDAS[19] `geomap` task. By applying the `geotran` task to the *Magellan* frame, and blinking this transformed image against the WFPC2 frames, we verified the quality of the registration. The `geoxytran` task then yielded the *x*, *y* pixel location of SPIRITS 15c in the *HST* images. The standard deviations of the geometric fits for the reference stars were 0.50 and 0.48 pixels in each coordinate in F555W and F814W, respectively, corresponding to 0.″05.

The precise location of SPIRITS 15c is shown in the upper right panel of Figure 1, with 3- and 5-σ error circles overlaid on the F555W image. At the pre-eruption site in 1998, we detect no progenitor star in either F555W or F814W. The location is within a dark dust lane, with very few stars detected in its vicinity. The 5-σ limiting magnitudes in the *HST* frames are $V > 25.1$ and $I > 24.0$ mag. These correspond to absolute magnitudes of $M_V > -7.9$ and $M_I > -8.9$ mag at the assumed distance of IC 2163, correcting only for Galactic extinction.

To analyze the location of this transient, we performed the same analysis on the Baade/IMACS image from 2014 February 6.2 with a clear detection of SPIRITS 14buu. Again, we found the standard deviations of the geometric fits for the reference stars were ≈0.50 pixels (≈0.″05) in each coordinate in both the F555W and F814W frames. The precise location of SPIRITS 14buu is shown in the right panel of Figure 1. The transient is coincident with a poorly resolved stellar association or cluster in the center of a dusty spiral arm, but it is not possible to identify an individual star as a candidate progenitor given the distance to IC 2163.

2.5. NIR Spectroscopy

We obtained an epoch of NIR spectroscopy of SPIRITS 15c with the Folded-port InfraRed Echellette spectrograph (FIRE; Simcoe et al. 2008, 2013) on the *Magellan* Baade Telescope at LCO at $t = 205$ days on 2015 March 14, and a later epoch with the Multi-object Spectrometer for Infra-red Exploration (MOSFIRE; McLean et al. 2010, 2012) on the Keck I Telescope at W. M. Keck Observatory at $t = 222$ days on 2015 March 31. SPIRITS 14buu was also included in the MOSFIRE slit mask, but the source was not detected above the host galaxy light. This was 60 days after the du Pont/Retrocam non-detection of SPIRITS 14buu at $J > 20.6$ mag.

The Baade/FIRE observations were obtained using the low-dispersion, high-throughput prism mode and a completed ABBA dither sequence. The data span 0.8–2.5 μm, at a resolution ranging from 300 to 500. Immediately afterward, we obtained a spectrum of the flux and telluric standard star HIP 32816. The data were reduced using the IDL pipeline FIREHOSE, which is specifically designed to reduce FIRE data (Simcoe et al. 2013). The pipeline performed steps of flat-fielding, wavelength calibration, sky subtraction, spectral tracing, and extraction. The sky flux was modeled using off-source pixels, as described by Kelson (2003), and was subtracted from each frame. The spectral extraction was then performed using the optimal technique of Horne (1986) to deliver the maximum signal-to-noise ratio while preserving spectrophotometric accuracy. Individual spectra were then combined with sigma clipping to reject spurious pixels. Corrections for telluric absorption were performed using the IDL tool *xtellcor* developed by Vacca et al. (2003). To construct a telluric correction spectrum free of stellar absorption features, a model spectrum of Vega was used to match and remove the hydrogen lines of the Paschen and Brackett series from the A0V telluric standard, and the resulting telluric correction spectrum was also used for flux calibration.

The Keck/MOSFIRE observations were carried out using 180 s exposures in the *Y*- and *K*-bands and 120 s exposures in *J* and *H*. The target was nodded along the slit between exposures to allow for accurate subtraction of the sky background. Total integration times in each band were 1431.5 s in *Y*, 715.8 s in *J*, 1192.9 s in *H*, and 1079.6 s in *K*. Spectral reductions, including flat-fielding, the wavelength solution, background

[19] STSDAS (Space Telescope Science Data Analysis System) is a product of STScI, which is operated by AURA for NASA.

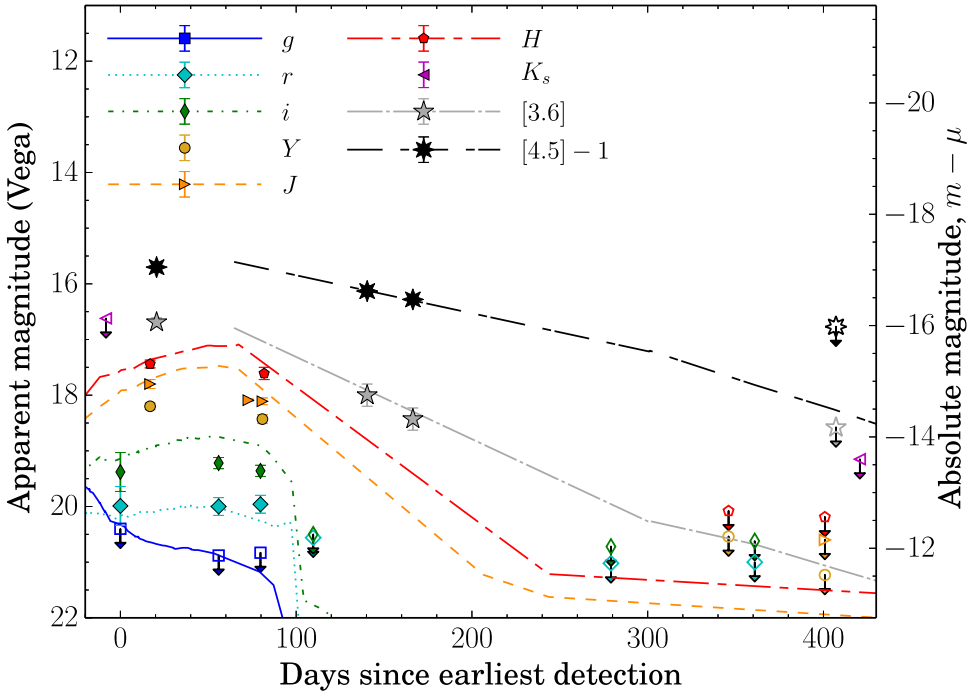

Figure 3. Optical (*gri*; AB magnitudes), and IR (*YJH*, [3.6], and [4.5]; Vega magnitudes) light curves of SPIRITS 14buu (points). Also shown are the *griJH* light curves of the Type IIP SN 2005cs and the [3.6] and [4.5] light curves of SN 2004et (lines). Unfilled points with downward arrows indicate upper limits. Error bars are shown, but are usually smaller than the points. Time on the *x*-axis is given as the number of days since the earliest detection of SPIRITS 14buu on MJD = 56650.3. The light curves of SN 2005cs are shifted in absolute magnitude by 0.1 mag, with applied total reddening characterized by $E(B-V) = 0.49$, or $A_V \approx 1.5$ mag assuming a standard $R_V = 3.1$ extinction law (Fitzpatrick 1999; Chapman et al. 2009; Schlafly & Finkbeiner 2011). The light curves of SN 2004et are shifted fainter by 2.4 mag. The phase of the SN 2005cs light curves is set so that fall-off of the plateau lines up with that of SPIRITS 14buu. The phase of the SN 2004et light curves is time in days from the assumed explosion epoch (MJD = 53270.0; Li et al. 2005).

subtraction, and frame stacking, were performed using the MOSFIRE Data Reduction Pipeline. 1D spectra were extracted from the 2D frames using standard tasks in IRAF. The A0V telluric standard HIP 30090 was also observed immediately following the observations of SPIRITS 15c and telluric corrections and flux calibrations were performed using *xtellcor*. The 1D spectra are shown in Figure 4, shifted to the rest frame of the ^{12}CO ALMA velocity measurements at the position of SPIRITS 15c (discussed in Section 2.1).

3. Analysis

In this section, we provide our analysis of the observed spectral energy density (SED) evolution of SPIRITS 15c and of its NIR spectrum.

3.1. The Optical to IR SED

We constructed a spectral energy distribution (SED) of SPIRITS 15c at multiple epochs ($t = 39$, 63, 106, 161, and 167 days) during the evolution of the transient using the available optical and IR photometry. The photometric points, converted to band-luminosities (λL_λ) assuming a distance to the host galaxy of 35.5 Mpc and correcting for galactic reddening, are shown in Figure 5 along with blackbody fits to the data at each epoch. To convert the *gri* optical points, we use AB flux zero points and broadband effective wavelengths for the SDSS filter system (Fukugita et al. 1996). For the *Y*-band, we adopt a Vega zero point of $f_\lambda = 5.71 \times 10^{-10}$ erg s^{-1} cm^{-2} Å^{-1} and an effective wavelength of $\lambda = 1.0305$ μm from Hewett et al. (2006). We adopt 2MASS system values from Cohen et al. (2003) for our *JHK*$_s$ photometry. For the *Spitzer* [3.6] and [4.5] points, we use the flux zero points and effective wavelengths listed in the IRAC instrument handbook for each channel.

At $t = 39$ days, the optical points are well-approximated by a blackbody with $T \approx 3300$ K and $R \approx 1.4 \times 10^{15}$ cm. Fits to the NIR points seem to indicate that the SED evolves in time to a higher effective temperature and smaller radius, with $T \approx 3500$ K and $R \approx 6.3 \times 10^{14}$ cm by $t = 106$ days. At $t = 161$–167 days, the SED shows at least two distinct components, with the NIR points approximated by a $T \approx 2700$ K, $R \approx 5.7 \times 10^{14}$ cm blackbody and a required cooler component to account for the [3.6] and [4.5] *Spitzer*/IRAC measurements, likely associated with dust emission. A blackbody fit to the measured band-luminosities at [3.6] and [4.5] gives a color temperature of $T \approx 270$ K. We note, however, that the sum of these two components significantly over-predicts the luminosity at [3.6].

Given that SPIRITS 15c coincides with an apparently dusty region of IC 2163, the observed SED is likely affected by significant extinction from host Galaxy dust. Thus, it is difficult to infer intrinsic properties of the transient from our photometric data. In Table 3, we give the results of blackbody fits to the data assuming several different values for the total extinction.

3.2. The NIR Spectrum

SPIRITS 15c was observed spectroscopically in the NIR at $t = 205$ and 222 days, during the IR decline phase of the transient. As seen in Figure 4, a prominent feature in both spectra is the broad emission line near 1.083 μm, most likely due to He I. The full-width at half-maximum (FWHM) velocity

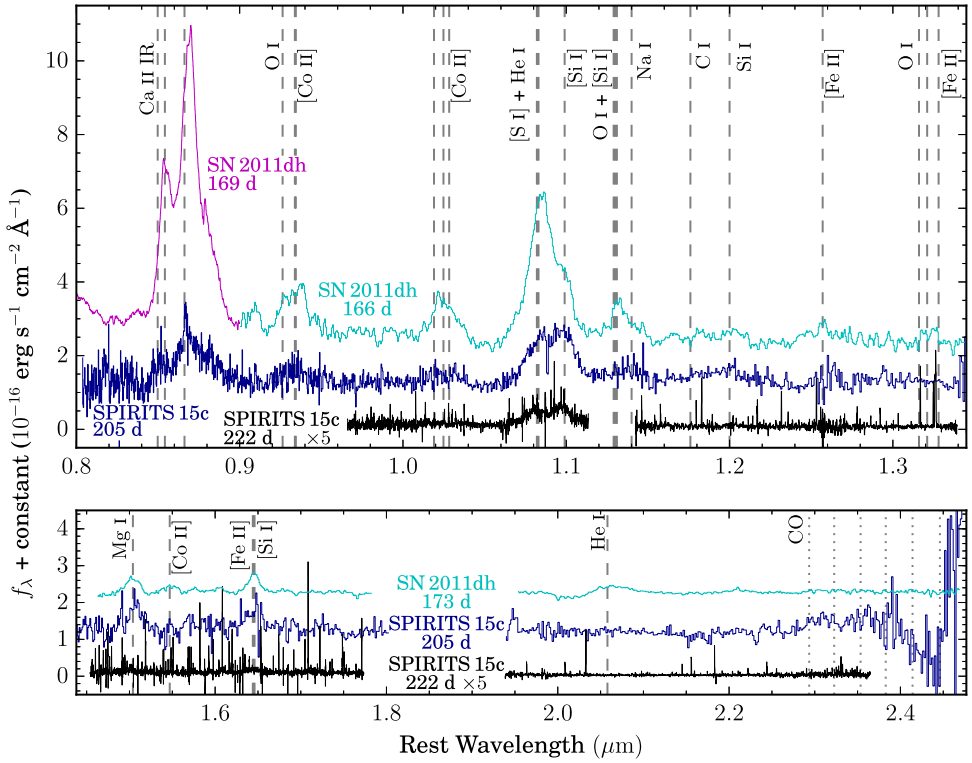

Figure 4. NIR spectra of SPIRITS 15c taken with Baade/FIRE on $t = 205$ days (blue) and Keck/MOSFIRE on $t = 222$ days (black) shifted to the rest frame of the the location of SPIRITS 15c measured in an ALMA CO velocity map of IC 2163 ($v_{\rm CO,helio} = 2827$ km s^{-1}, Elmegreen et al. 2016; Kaufman et al. 2016). The spectra are dereddened for galactic extinction, assuming a Fitzpatrick (1999) $R_V = 3.1$ extinction law. The Keck/MOSFIRE spectrum is multiplied by a factor of five and the Baade/FIRE spectrum is shifted up by 10^{-16} erg s^{-1} cm^{-2} Å^{-1} for clarity. We also show late-time spectra of SN 2011dh for comparison (cyan and magenta), shifted up by 2×10^{-16} erg s^{-1} cm^{-2} Å^{-1}, where the phases marked on the plot are set as in Figure 2. Dashed vertical lines show the locations of atomic transitions identified in the spectra of SN 2011dh by Ergon et al. (2014, 2015) and Jerkstrand et al. (2015). Dotted vertical lines mark the band heads of the $\Delta v = 2$ vibrational overtones of ^{12}C^{16}O, which may contribute to excess flux observed between 2.3 and 2.5 μm. The gaps in the spectra are due to the regions of low atmospheric transmission between the *J*, *H*, and *K* windows.

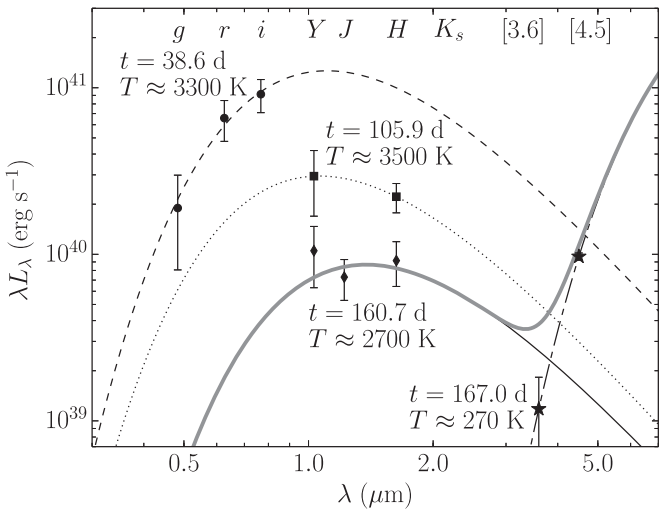

Figure 5. Optical-to-IR SED of SPIRITS 15c at multiple epochs during the evolution of the transient. Band-luminosities (λL_λ), calculated assuming a distance to IC 2163 of 35.5 Mpc and correcting for galactic reddening characterized by $E(B - V) = 0.072$ mag, are shown at $t = 38.6$ (circles), 105.9 (squares), 160.7 (diamonds), and 167.0 days (stars). Best-fit, single-component blackbody curves are shown as black dashed, dotted, dashed–dotted, solid, and long-short dashed lines, respectively, with their corresponding temperatures labeled. Because the final two epochs are nearly contemporaneous ($\Delta t = 6.3$ days), we show the sum of these two blackbody components as the solid gray curve.

of this line at $t = 166$ days is ≈8400 km s^{-1}. The line profile is shown in Figure 6, with a clear double-peaked structure that may indicate a high-velocity, bipolar outflow, or a toroidal geometry. The blueward peak also appears relatively weaker compared to the red side in the second epoch, and the full profile has narrowed to a FWHM velocity of ≈7600 km s^{-1}. The lower S/N of the second spectrum, however, adds difficulty to evaluating the significance of the profile evolution between the two epochs. In the FIRE spectrum, the narrow (FWHM ≈ 300 km s^{-1}), redshifted dip in the profile is likely an artifact. This dip is only two pixels wide, and narrower than a resolution element ($R_{\rm FIRE} = 500$). Moreover, it is not detected in the higher-resolution MOSFIRE spectrum ($R_{\rm MOSFIRE} = 3400$).

The flux in this line appears to have faded by a factor of more than 10 during the 17 days between the first and second epochs. Extrapolating from the observed *Y*-band decay rate of 0.020 ± 0.005 mag day^{-1} between 106 and 161 days, however, we would only expect the flux to have faded by a factor of ≈1.4. We caution that the spectral flux calibrations using standard star observations are somewhat uncertain, and we do not have contemporaneous photometric data to verify the fading of this line. Slit losses due to a misalignment may also contribute to the apparent drop in flux of the He I line, rather than true variability, in this feature. This could also explain the lack of detection of the continuum emission or any other features in the MOSFIRE spectrum.

Table 3
Parameters of SED Component Blackbody Fits

Phase[a] (days)	Total Extinction[b], A_V (mag)	$T_{\rm eff}$ (K)	$R_{\rm BB}$ (cm)
39	0.238	3300	1.4×10^{15}
	1.0	3800	1.3×10^{15}
	2.0	4600	1.1×10^{15}
	2.2	4900	1.1×10^{15}
	3.0	5900	9.6×10^{14}
106	0.238	3500	6.3×10^{14}
	1.0	3700	6.2×10^{14}
	2.0	4000	6.1×10^{14}
	2.2	4100	6.1×10^{14}
	3.0	4400	5.9×10^{14}
161	0.238	2700	5.7×10^{14}
	1.0	2800	5.5×10^{14}
	2.0	3100	5.3×10^{14}
	2.2	3200	5.2×10^{14}
	3.0	3400	5.1×10^{14}
167	0.238	270	3.7×10^{17}
	1.0	270	3.7×10^{17}
	2.0	270	3.6×10^{17}
	2.24	270	3.6×10^{17}
	3.0	270	3.5×10^{17}

Notes.
[a] Phase is number of days since the earliest detection of this event on 2014 August 21.4 (MJD = 56890.4).
[b] Assumed total extinction to SPIRITS 15c including both Galactic ($A_V = 0.238$), and any additional extinction, e.g., from the host environment.

The identification of the 1.083 μm line is somewhat uncertain because we do not detect the He I line at 2.058 μm in either spectrum. It is possible that there is a contribution to the red wing of the 1.083 μm feature from the Pa γ 1.094 μm line, but we do not detect Pa β or Pa δ (1.282 and 1.005 μm, respectively), indicating that H I is absent from the spectrum at this phase. Alternatively, it is possible that the two-component velocity profile is instead due to two distinct transitions: the [S I] 1.082 μm line for the blueward component, and the [Si I] 1.099 μm line for the redward component.

We also identify the blended 0.85 μm feature as the Ca II IR triplet (0.845, 0.854, and 0.866 μm). Without concurrent optical spectroscopy, we are unable to definitively identify any other features present in the $t = 205$ day spectrum of SPIRITS 15c. Also shown in Figure 4 are the NIR spectra of the Type IIb SN 2011dh at phases of ≈170 days, which show evident similarity to those of SPIRITS 15c. In addition to the broad, prominent He I line at 1.083 μm, we make tentative identifications of several other features in the spectra of SPIRITS 15c based on this comparison, including the blended O I and [Co II] feature near 0.93 μm, the [Co II] feature near 1.02 μm, the Mg I line at 1.504 μm, and the feature near 1.64 μm due to either [Fe II] or [Si I]. We list these identifications in Table 4, and discuss a detailed comparison between the NIR spectra of SPIRITS 15c and SN 2011dh below, in Section 4.1.1.

4. Discussion

Here, we discuss possible physical interpretations of SPIRITS 15c and SPIRITS 14buu and compare them to other classes of transients discovered in recent years.

Table 4
Spectral Line Identifications[a,b]

Species	Rest Wavelength (air) (μm)
He I	1.083
	2.058
C I	1.175
O I	0.926
	1.129
	1.130
	1.317
Na I	1.140
Mg I	1.504
Si I	1.203
[Si I]	1.099
	1.129
	1.646
[S I]	1.082
Ca II	0.845
	0.854
	0.866
[Co II]	0.934
	0.934
	1.019
	1.025
	1.028
	1.547
[Fe II]	1.257
	1.321
	1.328
	1.644
$^{12}C^{16}O$	2.294
	2.323
	2.354
	2.383
	2.414
	2.446

Notes.
[a] Line identifications come from Ergon et al. (2014, 2015), and Jerkstrand et al. (2015).
[b] Wavelengths listed for $^{12}C^{16}O$ correspond to band heads of the $\Delta v = 2$ vibrational overtones of this molecule.

4.1. SPIRITS 15c as an Obscured SN: Comparison with SN 2011dh

We examine the possibility that SPIRITS 15c is an SN explosion with significant obscuration by dust. We compare the properties of SPIRITS 15c to the well-studied Type IIb explosion in M51, SN 2011dh, based on the similarity of their NIR spectra at late phases (Section 4.1.1). Throughout this section, following Ergon et al. (2014), we adopt a median value from the literature for the distance to M51 of $7.8^{+1.1}_{-0.9}$ Mpc, and a reddening along the line of sight to SN 2011dh of $E(B - V) = 0.07$ mag assuming a standard $R_V = 3.1$ Milky Way extinction law as parametrized by Fitzpatrick (1999).

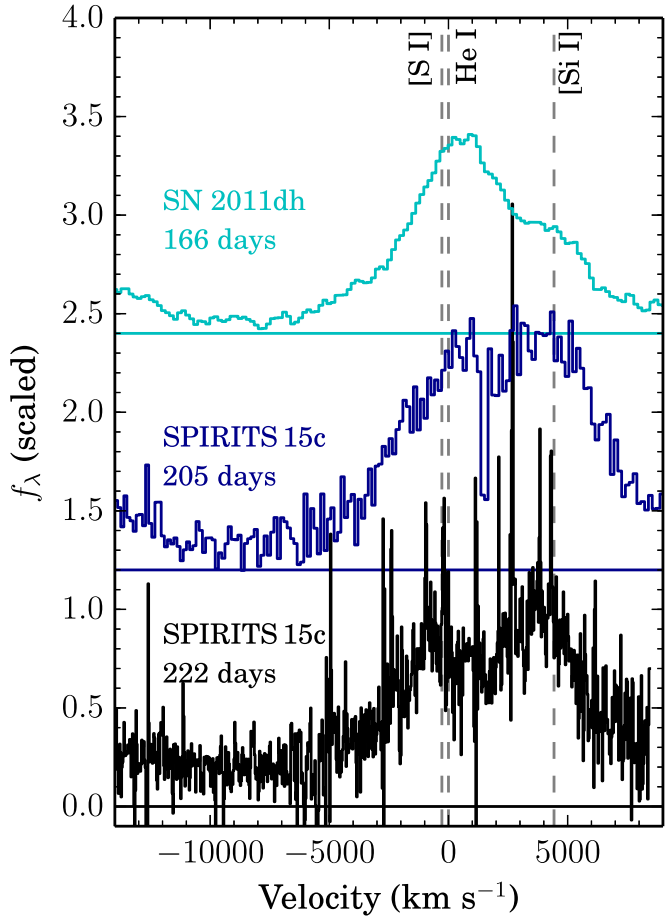

Figure 6. Observed velocity profile of the He I line at 1.0830 μm in the spectra of SN 2011dh at a phase of 166 days (top), and SPIRITS 15c at phases of 205 (middle) and 222 days (bottom). The phase of the SN 2011dh spectrum is set as in Figure 2. The profiles are scaled and shifted arbitrarily in flux for clarity.

4.1.1. NIR Spectrum Comparison

The NIR spectrum of SPIRITS 15c at $t = 205$ d shows pronounced similarity to the NIR spectra of SN 2011dh at similar phases. We show a direct comparison between the spectra of these objects in Figure 4, where the phase of the SN 2011dh spectra is set so that the earliest detection of the SN coincides with the most constraining non-detection preceding the outburst of SPIRITS 15c. The SN 2011dh spectra, originally published in Ergon et al. (2015), were obtained from the Weizmann Interactive Supernova data REPository (WISeREP, Yaron & Gal-Yam 2012).[20] To aid in the comparison, we mark the features identified in the spectra of SN 2011dh by Ergon et al. (2015) and Jerkstrand et al. (2015) in the figure.

A prominent feature in the spectra of both objects is the strong, broad ($\gtrsim$8000 km s^{-1}) He I emission at 1.083 μm, shown in detail in Figure 6. This line is detected in both spectra of SPIRITS 15c at $t = 205$ and 222 days. Ergon et al. (2015) note a blueshifted P-Cygni absorption component of this line profile in the SN 2011dh spectrum, extending to a velocity of at least $\approx$10,000 km s^{-1}, that may also be present in the line profile of SPIRITS 15c at $t = 202$ days. The He I line profile of SPIRITS 15c has a clear double-peaked structure that is not observed in SN 2011dh. This may suggest a bipolar outflow or toroidal geometry in SPIRITS 15c. We note that double-peaked [O I] lines present in many stripped-envelope CCSNe have been interpreted as evidence for a toroidal or disk-like geometry (e.g., Maeda et al. 2002, 2008; Mazzali et al. 2005; Modjaz et al. 2008; Milisavljevic et al. 2010). The shoulder feature on the red side of the SN 2011dh line profile, likely due to contamination from the [Si I] feature at 1.099 μm, may contribute to the redshifted peak of the line profile in SPIRITS 15c.

The He I line at 2.058 μm, detected in the spectrum of SN 2011dh, is not detected in either spectrum of SPIRITS 15c. Assuming the same flux ratio between the 1.083 and 2.058 μm He I lines as is observed in SN 2011dh, and accounting for additional reddening as inferred for SPIRITS 15c (in Section 4.1.3), we would expect the 2.058 μm He I to peak at 0.09×10^{-16} erg s^{-1} cm^{-2} Å^{-1} above the continuum in the FIRE spectrum. This is below the rms noise of 0.11 erg s^{-1} cm^{-2} Å^{-1} in this region of the spectrum, and thus, a non-detection of this feature is not surprising.

Other prominent emission features detected in the spectra of both objects include the Ca II IR triplet, the blended features due to O I and [Co II] near 0.93 μm, the [Co II] feature near 1.02 μm, the Mg I line at 1.504 μm, and the feature near 1.64 μm due to [Fe II] or [Si I]. We caution, however, that the NIR line identifications for SN 2011dh by Ergon et al. (2014, 2015) and Jerkstrand et al. (2015) relied on corroborating detections in the optical. We do not have optical spectroscopy of SPIRITS 15c to confirm the identifications of these features.

The excess emission beyond 2.3 μm, attributed to the $\Delta v = 2$ vibrational overtones of CO by Ergon et al. (2015) and Jerkstrand et al. (2015), in the spectrum of SN 2011dh appears even stronger in SPIRITS 15c, but we note that the spectrum of SPIRITS 15c becomes increasingly noisy beyond $\approx$2.4 μm at the end of K-band. Some of the weaker spectral features, labeled in Figure 4 and present in the spectrum of SN 2011dh, are not detected in SPIRITS 15c, but this can likely be accounted for by the relatively lower S/N of the SPIRITS 15c spectra, small intrinsic differences in the strength of these features between the two events, and the uncertainty of matching the evolutionary phase between the two events. Overall, we find that the late-time, NIR spectrum of SN 2011dh provides a good match to the spectra of SPIRITS 15c, and we evaluate the interpretation of SPIRITS 15c as a Type IIb SN similar to SN 2011dh, albeit subject to significant dust obscuration, below in Sections 4.1.2 and 4.1.3.

4.1.2. Progenitor Comparison

As discussed above in Section 2.4, no progenitor star was detected at the position of SPIRITS 15c in pre-explosion *HST* imaging of IC 2163 and NGC 2207 to limiting magnitudes of $M_V > -7.9$ and $M_I > -8.9$ mag at the assumed distance to the host, correcting only for galactic extinction. A candidate progenitor of SN 2011dh was identified as an intermediate-mass yellow supergiant star in pre-explosion *HST* images at the position of the SN (Maund et al. 2011; van Dyk et al. 2011). The disappearance of this source in post-explosion imaging confirms that it was the progenitor star (van Dyk et al. 2013; Ergon et al. 2014). The observed magnitudes in the *HST* frames were $V \sim 21.8$ and $I \sim 21.2$, corresponding to absolute magnitudes of $M_V \sim -7.9$ and $M_I \sim -8.4$ at the assumed distance, and reddening to SN 2011dh (Maund et al. 2011;

[20] WISeREP spectra are available here: http://wiserep.weizmann.ac.il/.

van Dyk et al. 2011). These values are consistent with the non-detection of a progenitor star for SPIRITS 15c in the archival *HST* imaging of IC 2163, and furthermore, there may be significant, additional extinction from the foreground spiral arm of NGC 2207 and the local environment of the transient. Thus, we cannot rule out a progenitor system similar to that of SN 2011dh for SPIRITS 15c.

4.1.3. Light Curve and SED Comparison

The optical and IR light curves of SPIRITS 15c are shown in Figure 2. The peak observed brightness of the transient in the optical was in *i*-band at $i = 17.67 \pm 0.09$ mag ($M_i = -15.08$ mag absolute). The peak in *i*-band absolute magnitude of SN 2011dh was brighter by ≈2 mag, possibly indicating that SPIRITS 15c is subject to significant dust extinction. To examine this scenario, we compare the light curves of SN 2011dh from Helou et al. (2013), Ergon et al. (2014, 2015) to those of SPIRITS 15c in Figure 2. The light curves of SN 2011dh have been shifted in apparent magnitude to the assumed distance of SPIRITS 15c, and are shifted in phase so that the earliest detection of SN 2011dh coincides with the last non-detection of SPIRITS 15c before its outburst. We then applied a Fitzpatrick (1999) extinction law with $R_V = 3.1$ and $E(B-V) = 0.72$ mag, corresponding to $A_V = 2.2$ mag, to the SN 2011dh light curves. As shown in the figure, this provides a good match to the observed magnitudes of SPIRITS 15c in *gri* at $t = 38.6$ days. We note a few small discrepancies with the optical light curves in this comparison. Namely, SPIRITS 15c is fainter than the adjusted brightness of SN 2011dh at $t = 0$ days in *i*-band by ≈0.3 mag, and brighter by ≈0.1 mag at $t = 30$ days.

Although the reddened light curves of SN 2011dh provide a good match to the optical light curves of SPIRITS 15c, the IR light curves are more difficult to explain using only a standard extinction law. For the extinction and phase assumed for SN 2011dh in Figure 2, several discrepancies are apparent. At $t = 106$ days, the *H*-band magnitude is brighter than the corresponding value for SN 2011dh by 0.6 mag. Furthermore, the SN 2011dh *H*-band light curve decays faster, resulting in a larger discrepancy of 1.0 mag by $t = 161$ days. At the same phase, the adjusted magnitude of SN 2011dh is 0.9 mag fainter than that of SPIRITS 15c in *J*. The single K_s-band detection of SPIRITS 15c at 181 days matches the reddened light curve of SN 2011dh quite well.

The largest discrepancy occurs in the *Spitzer*/IRAC [3.6] and [4.5] bands. In [4.5], the SPIRITS 15c light curve is brighter than that of SN 2011dh by ≈0.4 mag between $t = 167$ and 307 days, although they decay at similar rates. However, in [3.6] at $t = 167$ days, SPIRITS 15c is fainter than the reddened SN 2011dh by 1.5 mag. To explain the 1.9 mag excess in [3.6]–[4.5] color of SPIRITS 15c over SN 2011dh, using only a standard reddening law, would require $\gtrsim$100 mag of visual extinction.

We make a similar comparison between the SED of SPIRITS 15c and the reddened SED of SN 2011dh at several phases in Figure 7. As in the light curve comparison, we find that applying extinction with $E(B-V) = 0.72$ to the SED of SN 2011dh at $t = 39$ and 63 days does a good job of reproducing the observed optical *gri* band-luminosities of SPIRITS 15c. The IR *YJH*, and [4.5] band-luminosities, however, are significantly over-luminous compared to the reddened SN 2011dh between $t = 106$ and 307 days. Again, the most apparent discrepancy in this comparison is the

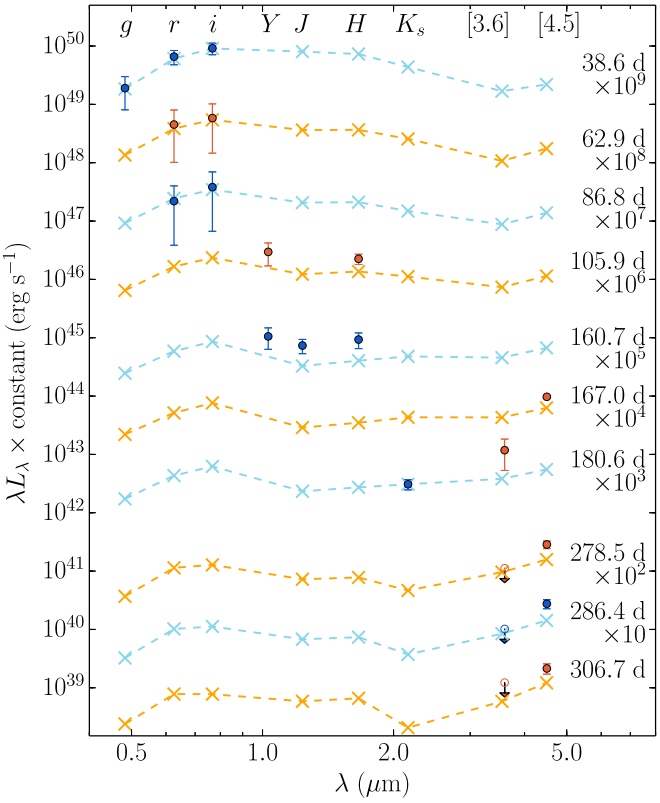

Figure 7. Comparison of the SED evolution of SPIRITS 15c (dark blue/orange circles) and SN 2011dh (light blue/orange "X"-symbols). Unfilled points with downward arrows represent upper limits. The band luminosities for SPIRITS 15c are corrected for galactic extinction to IC 2163 from NED (Fitzpatrick 1999; Chapman et al. 2009; Schlafly & Finkbeiner 2011). The points for are SN 2011dh drawn from a linear interpolation of the SN 2011dh light curves, and reddened by the assumed excess extinction in SPIRITS 15c characterized by $E(B-V)_{\rm host} = 0.65$, with a standard $R_V = 3.1$ extinction law. Error bars for SPIRITS 15c are shown, but are sometimes smaller than the plotting symbols. The phase, set as in Figure 2, of each SED is listed along the right side. Each SED is shifted up by a factor of 10 from the one below, in alternating colors, so that they can be easily distinguished.

significant over-prediction of the luminosity of SPIRITS 15c at [3.6].

Because SPIRITS 15c appears over-luminous in some bands, and under-luminous in others, compared to the reddened light curves and SED of SN 2011dh, a phase shift in the light curves of SN 2011dh cannot account for the observed discrepancies. Furthermore, using a steeper or shallower extinction law to redden the observations of SN 2011dh would be unable to rectify all of the observed discrepancies at once.

4.1.4. SPIRITS 15c in the Context of SNe IIb

The designation IIb indicates an SN that transitions spectroscopically from a hydrogen-rich SN II to a hydrogen-poor SN Ib. These events are believed to arise from the core collapse of massive stars that have been stripped of almost all of their hydrogen envelope. In addition to SN 2011dh, well-studied examples of SNe IIb include SN 1993 J and SN 2008ax.

The progenitor of SN 1993 J was shown to be a yellow supergiant star of 12–17 $M_\odot$, similar to that of SN 2011dh. It was proposed to have lost most of its hydrogen envelope to a blue, compact companion star (Podsiadlowski et al. 1993; Shigeyama et al. 1994; Woosley et al. 1994; Blinnikov et al. 1998;

Maund et al. 2004; Stancliffe & Eldridge 2009). The progenitor observations of SN 2008ax by Crockett et al. (2008) were less conclusive, but Tsvetkov et al. (2009) proposed a 13 $M_{\odot}$ star with an extended, low-mass hydrogen envelope, based on hydrodynamical modeling of the SN optical light curves. As mentioned above in Section 4.1.2, we do not rule out a progenitor similar to those of other SNe IIb based on pre-explosion *HST* imaging.

Ergon et al. (2014) showed that these SNe had similar optical light curve and color evolution in the first 50 days. All three reached peak luminosity at ≈20 days post explosion, and evolved to redder colors with time. They noted some differences between the three events, such as a factor of three spread in peak luminosity, and a ≈0.4 mag spread in their optical colors, but these differences could be accounted for within the systematic uncertainties in the distance and extinction to each SN. The assumption of $E(B-V)_{\rm host} = 0.65$ mag for SPIRITS 15c brings its optical light curves and color evolution into good agreement with the observed properties of well-studied SNe IIb.

The IR light curves of SPIRITS 15c are not as well-matched by a reddened version of SN 2011dh, but it is not as straightforward to draw a direct comparison between the two events at these wavelengths. SN 2011dh was shown to have a significant IR excess at [4.5] compared to the NIR and [3.6] measurements, possibly due to a thermal echo from heated CSM dust, dust formation in the ejecta, and/or CO fundamental band emission (Helou et al. 2013; Ergon et al. 2014, 2015). Similar confounding factors may be at play in SPIRITS 15c, given the observed excess at NIR wavelengths and at [4.5], and the possible CO $\Delta v = 2$ vibrational emission present in the *K*-band spectrum. The extreme [3.6]–[4.5] = 3.0 ± 0.2 mag color of SPIRITS 15c at a phase of 167 days has not been observed for another SN IIb, and provides the strongest challenge to the interpretation of SPIRITS 15c as a moderately obscured SN 2011dh-like event. SN 2011dh only reached a *Spitzer*/IRAC color of 1.6 mag at ≈400 days, and the Type IIb SN 2013df was observed to have a 1.3 mag color at ≈300 days (Tinyanont et al. 2016).

Although SPIRITS 15c and SN 2011dh show remarkable similarity in many respects, we note that we do not have sufficient data for this case to discriminate between an SN IIb or SN Ib. As is clearly demonstrated by Fremling et al. (2016), the light curves of PTF 12os (Type IIb SN 2012P) and PTF 13bvn (Type Ib SN) show only very minor differences to each other and to SN 2011dh. Spectroscopically, SNe Ib and IIb are only distinguished by the presence or absence of hydrogen in their early-time spectra. The absence of hydrogen in the spectrum of SPIRITS 15c after ≈200 days does not classify this event as a SN Ib, as hydrogen may very well have been present at earlier times.

4.2. SPIRITS 14buu: Yet Another Reddened SN?

The optical light plateau and subsequent fall-off observed for SPIRITS 14buu are similar to those characteristic of the SN IIP class of CCSNe. The duration of SNe IIP plateaus is typically ≈100 days (e.g., Poznanski et al. 2009; Arcavi et al. 2012). Sanders et al. (2015) found, using a statistical sample of SN IIP light curves from Pan-STARRS1, a median *r*-band plateau duration of 92 days, with a 1σ variation of 14 days, although the full distribution spanned a range of 42–126 days. The observed >80 day plateau of SPIRITS 14buu in the *r* and *i* bands is thus consistent with the observed distribution for SNe IIP.

SNe IIP have been observed to exhibit a wide-ranging continuum in observed peak magnitude in the optical ($-14.5 \gtrsim M_r \gtrsim -20.0$, $-15.0 \gtrsim M_i \gtrsim -19.5$, Sanders et al. 2015), with higher-luminosity events exhibiting greater expansion velocities and producing larger amounts of nickel (e.g., Hamuy 2003). Correcting only for galactic extinction, SPIRITS 14buu is fainter than the faintest SN IIP in the Sanders et al. (2015) sample by ≈1.5 mag in both the *r* and *i* bands. It is possible that IC 2163 is an intrinsically low-luminosity SN IIP; however, the observed red colors may also indicate additional dust extinction.

To examine this possibility, we compare SPIRITS 14buu to the low-luminosity Type IIP SN 2005cs in M51 in Figure 3. We obtained *BVRIJH* light curves of SN 2005cs from Pastorello et al. (2009). For extinction, we assume their value to be $E(B-V) = 0.05$ mag. For a direct comparison, the optical measurements were converted to SDSS system magnitudes using the conversions from (Jordi et al. 2006), and corrected for galactic extinction to M51. Following a method similar to that used in Section 4.1.3, we then shifted the SN 2005cs light curves in apparent magnitude to the distance of IC 2163, and applied a total reddening characterized by $E(B-V) = 0.49$ mag with a standard $R_V = 3.1$ Fitzpatrick (1999) extinction law, corresponding to 1.5 mag of visual extinction. We also shifted SN 2005cs light curves by an additional 0.1 mag (smaller than the uncertainties in the distance moduli to the hosts) to achieve a better match to the *r* and *H*-band measurements for SPIRITS 14buu. The phase of SN 2005cs was set so that the fall-off of the optical plateau coincides with that of SPIRITS 14buu.

The reddened light curves of SN 2005cs provide a good match to the *r*, *J*, and *H*-band light curves of SPIRITS 14buu. The *g*-band upper limits for SPIRITS 14buu are also mostly consistent with the reddened *g*-band light curve of SN 2005cs. The largest discrepancy is in the *i*-band between 60 and 100 days, where SPIRITS 14buu is 0.5 mag fainter than the reddened SN 2005cs.

We also compare the [3.6] and [4.5] light curves of SPIRITS 14buu to those of the Type IIP SN 2004et from Kotak et al. (2009), in Figure 3. The SN 2004et light curves are shifted fainter in absolute magnitude by 2.4 mag, to match the level of SPIRITS 14buu. This also suggests that SPIRITS 14buu may be an intrinsically faint event like SN 2005cs, in addition to suffering from significant extinction. The decay rate of SN 2004et is somewhat faster than SPIRITS 14buu in both *Spitzer*/IRAC bands. Tinyanont et al. (2016) present a sample of SN light curves at [3.6] and [4.5], and find that SN II MIR light curves show a large degree of variety. Thus, we would not necessarily expect to find a good match to the MIR of SPIRITS 14buu in the relatively small sample of SNe IIP that have been well-studied at these wavelengths.

Without a spectrum, we cannot definitively determine the nature of this source. Overall, however, we find a low-luminosity SN IIP, similar to SN 2005cs with ≈1.5 mag of visual extinction, to be a reasonable explanation for the observed properties of SPIRITS 14buu.

4.3. Non-SN IR Transient Scenarios

We also consider the possibility that SPIRITS 15c and SPIRITS 14buu are not obscured SNe. Below, we find that scenarios involving a stellar merger and an SN 2008S-like transient can likely be ruled out for both events. We also consider a V445 Pup-like helium nova, which can likely be ruled out in the case of SPIRITS 15c due to its high luminosity.

4.3.1. Stellar Merger

Known transients associated with stellar merger events include the low-mass (1–2 $M_{\odot}$) contact binary merger V1309 Sco (Tylenda et al. 2011), and the more massive merger of a B-type progenitor (5–10 $M_{\odot}$) V838 Mon (Bond et al. 2003; Sparks et al. 2008). Recently, the NGC 4490-OT has also been proposed to be a high-mass (20–30 $M_{\odot}$) analog of these events (Smith et al. 2016). The observed examples of stellar mergers are characterized by unobscured, optical progenitors; irregular, multi-peaked light curves; increasing red colors with time; and a significant IR excess at late times. The spectra during the decline phase show relatively narrow lines (O[10^2] km s^{-1}) of H I in emission and Ca II in absorption.

The light curve of SPIRITS 15c shows some similarities to the massive stellar merger NGC4490-OT, although it is ≈1–2 mag brighter both during the optical peak, and in the IR *Spitzer*/IRAC bands at late times. The [3.6]–[4.5] color of SPIRITS 15c is significantly redder. The optical outburst of the NGC 4490-OT lasted longer than 200 days and the IR light curve extends in excess of 800 days. SPIRITS 15c, in contrast, faded beyond detection in the optical in $\lesssim$150 days, and in the IR in $\lesssim$500 days. In the case of the NGC 4490-OT, the evidence for a massive stellar merger is corroborated by the detection of a massive progenitor at $M_{\rm F606W} \approx -6.4$, likely an $M \approx 30\ M_{\odot}$ LBV. This extends the observed correlation suggested by Kochanek et al. (2014) in peak luminosity and merger progenitor mass (Smith et al. 2016). Further extending this correlation to the luminosity of SPIRITS 15c would suggest an extremely massive progenitor ($M \gtrsim 60\ M_{\odot}$). The progenitor of SPIRITS 15c was undetected in the 1998 *HST* images to $M_V > -7.9$ mag. Furthermore, the velocities observed in SPIRITS 15c are $\gtrsim$10 times those seen in stellar mergers, indicating a significantly more explosive event. Finally, the lack of hydrogen observed for SPIRITS 15c would require a rare, very massive stripped-envelope system. Taken together, the evidence indicates that a massive stellar merger scenario is likely ruled out as an explanation for the properties of SPIRITS 15c.

SPIRITS 14buu reached a similar peak luminosity in the *i*-band to the peak optical luminosity of the NGC 4490-OT, but SPIRITS 14buu is ≈1 mag brighter at [4.5]. As with SPIRITS 15c, the NGC 4490-OT evolved much more slowly than SPIRITS 14buu in both the optical and IR. Furthermore, the observed plateau of SPIRITS 14buu in the optical is inconsistent with the characteristic multi-peaked light curves of stellar merger events. We find that, despite the similarity in observed optical luminosity, SPIRITS 14buu is overall inconsistent with an NGC 4490-OT-like stellar merger.

4.3.2. SN 2008S-like Transient

SN 2008S-like transients, including the 2008 luminous optical transient in NGC 300 (NGC 300 OT2008-1) and other similar events, are a class of so-called SN imposters. These events have highly obscured progenitors in the optical, but bright MIR detections ($M_{[4.5]} < -10$) suggest that the progenitors are likely extreme asymptotic giant branch stars of intermediate mass (≈10 to 15 $M_{\odot}$), self-obscured by a dense wind of gas and dust (Prieto et al. 2008; Bond et al. 2009; Thompson et al. 2009). They are significantly less luminous than SNe in the optical, with peak absolute visual magnitude of only $M_V \approx -13$ for SN 2008 S (Steele et al. 2008) and $M_V \approx -12$ to -13 for NGC 300 OT2008-1 (Bond et al. 2009). These events have peculiar spectral features, including narrow emission from [Ca II], Ca II, and weak Fe II (Steele et al. 2008; Bond et al. 2009; Humphreys et al. 2011). Moderate-resolution spectroscopy of NGC 300 OT2008-1 revealed that the emission lines showed a double-peaked structure, indicating a bipolar outflow with expansion velocities of ≈70–80 km s^{-1} (Bond et al. 2009; Humphreys et al. 2011). A proposed physical picture of these events is that a stellar explosion or massive eruption, possibly an electron-capture SN, destroys most of the obscuring dust, allowing the transient to be optically luminous. In the aftermath, however, the dust reforms and re-obscures the optical transient, producing a significant IR-excess (Thompson et al. 2009; Kochanek 2011). Both transients have now faded beyond their progenitor luminosities at [3.6] and [4.5], suggesting that the outbursts were terminal events (Adams et al. 2016).

The optical and late-time MIR luminosities of SPIRITS 15c are 1–2 mag brighter than is observed for SN 2008S-like events, and SPIRITS 15c is again significantly redder in the MIR (only ≈1 mag for SN 2008S-like events, Szczygieł et al. 2012). As with SN 2008 S and the NGC 300 OT2008-1, the progenitor of SPIRITS 15c was obscured in the optical. There was no detection of a MIR progenitor for SPIRITS 15c down to ≈14.9 mag (≈−17.85 absolute), but this limit is not constraining due to the larger distance to IC 2163 and the bright background galaxy light in the vicinity of SPIRITS 15c. The observed velocities of SPIRITS 15c are much higher than those of SN 2008 S or the NGC 300 OT2008-1, which show similar velocities to stellar mergers. The strongest evidence against SPIRITS 15c as a SN 2008S-like event is the lack of hydrogen in its spectrum. SN 2008 S and the NGC 300 OT2008-1 both showed strong hydrogen emission features, and moreover, if the physical mechanism behind them is indeed an electron-capture SN, the lack of hydrogen in SPIRITS 15c would be inexplicable given the believed intermediate-mass progenitors of such events.

The *i*-band luminosity of SPIRITS 14buu is comparable to an SN 2008S-like event in the optical, and both SPIRITS 14buu and SN 2008 S reached IR luminosities of $M_{[4.5]} \approx -16$. SN 2008 S was also significantly redder in [3.6]–[4.5] color, by ≈0.8 mag. Additionally, SN 2008 S was fainter than SPIRITS 14buu in the NIR, by ≈2 mag. The largest discrepancy is that the optical light curves of SN 2008 S decayed steeply after only ≈30 days, in contrast with the $\gtrsim$80 day plateau of SPIRITS 14buu. Thus, we find an SN 2008S-like event to be a poor match to the observed properties of SPIRITS 14buu.

4.3.3. V445 Pup-like Transient or a Helium Nova

An intriguing possibility for an explanation of SPIRITS 15c is a helium nova, a rare and thus far largely theoretical class of events. Helium novae are due to thermonuclear runaway on the surface of a white dwarf accreting helium from a helium-rich donor (Kato et al. 1989). The most convincing and well-studied candidate for an observed helium nova is the 2000 outburst of

the galactic object V445 Pup. The optical outburst showed a similar decline to slow novae, but was small in amplitude, with $\Delta m_V \approx 6$ mag. Its spectrum was also unusual for a classical nova, in that it was rich in He I and C I emission lines, but showed no evidence for hydrogen. Multi-epoch adaptive optics imaging and integral field unit spectroscopy revealed an expanding bipolar outflow from V445 Pup, with a velocity of $\approx$6700 km s^{-1} and some knots at even larger velocities of $\approx$8500 km s^{-1} (Woudt et al. 2009). Using their observations of the expanding shell, Woudt et al. (2009) derive an expansion parallax distance of 8.2 ± 0.5 kpc.

The broad, double-peaked He I line in the spectrum of SPIRITS 15c is in good agreement with the observed velocities of the bipolar helium outflow of V445 Pup. The largest problem with this scenario, however, is that the V445 Pup outburst was significantly less luminous than SPIRITS 15c in the optical, with a peak of only $M_V \approx -6$. The NIR of peak at $M_{K_s} \approx -10$ was more comparable to that of SPIRITS 15c, and both sources grew redder with time during the initial decline. Late-time observations of V445 Pup with *Spitzer*/IRAC in 2005 (P20100; PIs Banerjee & P. Dipankar) and 2010 (P61071; PI B. A. Whitney), approximately 5 and 10 years after the outburst, respectively, revealed the source was slowing decaying at [3.6] from $m_{[3.6]} \approx 8.6$ to 9.5 (-6 to -5.1 absolute) over $\approx$5 years. The source was saturated in the IRAC2, IRAC3, and IRAC4 channels, indicating very red lower limits on the MIR colors of [3.6]–[4.5] $\gtrsim$ 2.3 mag, [3.6]–[5.7] $\gtrsim$ 3.4 mag, and [3.6]–[7.9] $\gtrsim$ 4.2 mag.

5. Conclusions

SPIRITS 15c is a luminous ($M_{[4.5]} = -17.1 \pm 0.4$), red ($[3.6] - [4.5] = 3.0 \pm 0.2$ mag), IR-dominated transient discovered by the SPIRITS team. The transient was accompanied by an optical precursor outburst with $M_i = -15.1 \pm 0.4$ mag that was quickly overtaken by IR emission within $\approx$100 days. The most prominent feature of the NIR spectrum is a broad ($\approx$8000 km s^{-1}), double-peaked emission line at 1.083 μm, likely due to He I, possibly indicating a He-rich, bipolar, or toroidal outflow associated with the transient.

We explored several possible scenarios to explain the unusual observed properties of SPIRITS 15c. Both the stellar merger and SN 2008S-like scenarios can likely be ruled out by the high luminosity of SPIRITS 15c, as well as the explosive velocities and lack of hydrogen in its spectrum. In the case of a helium nova, the strong He I emission and high-velocity, bipolar outflow of SPIRITS 15c is similar to that observed in the candidate prototype helium nova V445 Pup, but again, the optical luminosity of SPIRITS 15c is too extreme.

We conclude that SPIRITS 15c is a stripped-envelope, CCSN explosion similar, to the well-studied Type IIb SN 2011dh, but extinguished by dust in the optical and NIR at a level of $A_V \approx 2.2$ mag. The spectrum of SPIRITS 15c is very similar to that of SN 2011dh at a phase of $\approx$200 days, but SPIRITS 15c shows a distinct double-peaked profile in the broad, strong He I emission line that is not observed in SN 2011dh. The assumption of $A_V = 2.2$ mag with a standard $R_V = 3.1$ extinction law in SPIRITS 15c provides a good match between the optical light curves and observed colors of SPIRITS 15c, and those of SN 2011dh. In the IR, however, SPIRITS 15c is more luminous than SN 2011dh, except at [3.6] where it is significantly under-luminous, illustrated by its extreme [3.6]–[4.5] color. Thus, we find that a shift in phase or simply a steeper extinction law cannot explain the observed differences between SPIRITS 15c and SN 2011dh.

SPIRITS 14buu, an earlier transient in IC 2163, was serendipitously discovered in the SPIRITS data during the analysis of SPIRITS 15c. The source was also luminous in the IR at $M_{[4.5]} = -16.1 \pm 0.4$ mag, and developed a fairly red [3.6]–[4.5] color of 1.2 ± 0.2 mag by 166 days after its first detection. The optical and NIR light curves showed a plateau lasting at least 80 days, similar to that observed in SNe IIP. Scenarios involving a stellar merger or SN 2008S-like transient can again likely be ruled out. A comparison to the low-luminosity Type IIP SN 2005cs, assuming $\approx$1.5 mag of visual extinction, produced a reasonable match to the properties of SPIRITS 14buu. We find an obscured SN IIP to be the most likely interpretation for SPIRITS 14buu considered here.

The key to fully understanding the nature of these events is MIR spectroscopy, the likes of which will become available with the launch of the *James Webb Space Telescope* (*JWST*). A MIR spectrum would, for example, enable us to elucidate the origin of the extreme [3.6]–[4.5] color observed in SPIRITS 15c, and identify spectral features contributing to the flux at these wavelengths, e.g., the fundamental vibrational overtones of CO that may contribute to the high luminosity at [4.5]. Moreover, photometric coverage further into the MIR with *JWST* would allow us to detect the presence of a cooler dust component than is accessible with the warm *Spitzer*/IRAC bands.

The census of SNe in nearby galaxies from optical searches, even at only 35 Mpc, is incomplete. In less than three years of monitoring nearby galaxies at IR wavebands, SPIRITS has discovered at least one, possibly two, moderately extinguished SNe that went unnoticed by optical surveys, SPIRITS 15c and SPIRITS 14buu. Since the start of the SPIRITS program, our galaxy sample has hosted nine optically discovered CCSNe. This may suggest a rate of CCSNe in nearby galaxies, missed by current optical surveys, of at least 10%. If SPIRITS 14buu is also indeed an SN, this estimate increases to 18%. In a future publication, we will present an analysis of the full SPIRITS sample of SN candidates to provide a more robust estimate of the fraction of SNe being missed by optical surveys. If this fraction is high, it could have significant implications for our understanding of the CCSN rate and its connection to star-formation rates. Additionally, the discovery of IR transients such as SPIRITS 15c and SPIRITS 14buu in a galaxy-targeted survey indicates that the night sky is ripe for exploration by dedicated wide-field, synoptic surveys in the IR.

We thank the anonymous referee for the comments that improved the manuscript. We thank M. Kaufman, B. Elmegreen, and the authors of Elmegreen et al. (2016) and Kaufman et al. (2016) for providing Hα, 24 μm, and CO measurements at the location of SPIRITS 15c. We also thank P. Groot, R. Lau, and S. Adams for valuable discussions.

This material is based upon work supported by the National Science Foundation Graduate Research Fellowship under grant no. DGE-1144469. H.E.B. acknowledges support for this work provided by NASA through grants GO-13935 and GO-14258 from the Space Telescope Science Institute, which is operated by AURA, Inc., under NASA contract NAS 5-26555. R.D.G. was supported in part by the United States Air Force.

This work makes use of observations from the LCO network. This paper includes data gathered with the 6.5 m *Magellan* Telescopes located at LCO, Chile.

This work is based in part on observations made with the *Spitzer Space Telescope*, which is operated by the Jet Propulsion Laboratory, California Institute of Technology under a contract with NASA. The work is based, in part, on observations made with the Nordic Optical Telescope, operated by the Nordic Optical Telescope Scientific Association at the Observatorio del Roque de los Muchachos, La Palma, Spain, of the Instituto de Astrofisica de Canarias.

Funding for the Sloan Digital Sky Survey IV has been provided by the Alfred P. Sloan Foundation, the U.S. Department of Energy Office of Science, and the Participating Institutions. SDSS-IV acknowledges support and resources from the Center for High-Performance Computing at the University of Utah. The SDSS web site is www.sdss.org.

SDSS-IV is managed by the Astrophysical Research Consortium for the Participating Institutions of the SDSS Collaboration including the Brazilian Participation Group, the Carnegie Institution for Science, Carnegie Mellon University, the Chilean Participation Group, the French Participation Group, Harvard-Smithsonian Center for Astrophysics, Instituto de Astrofísica de Canarias, The Johns Hopkins University, Kavli Institute for the Physics and Mathematics of the universe (IPMU)/University of Tokyo, Lawrence Berkeley National Laboratory, Leibniz Institut für Astrophysik Potsdam (AIP), Max-Planck-Institut für Astronomie (MPIA Heidelberg), Max-Planck-Institut für Astrophysik (MPA Garching), Max-Planck-Institut für Extraterrestrische Physik (MPE), National Astronomical Observatories of China, New Mexico State University, New York University, University of Notre Dame, Observatário Nacional/MCTI, The Ohio State University, Pennsylvania State University, Shanghai Astronomical Observatory, United Kingdom Participation Group, Universidad Nacional Autónoma de México, University of Arizona, University of Colorado Boulder, University of Oxford, University of Portsmouth, University of Utah, University of Virginia, University of Washington, University of Wisconsin, Vanderbilt University, and Yale University.

References

Adams, S. M., Kochanek, C. S., Prieto, J. L., et al. 2016, MNRAS, 460, 1645
Arcavi, I., Gal-Yam, A., Cenko, S. B., et al. 2012, ApJL, 756, L30
Blagorodnova, N., Kotak, R., Polshaw, J., et al. 2017, ApJ, 834, 107
Blinnikov, S. I., Eastman, R., Bartunov, O. S., Popolitov, V. A., & Woosley, S. E. 1998, ApJ, 496, 454
Bond, H. E. 2011, ApJ, 737, 17
Bond, H. E., Bedin, L. R., Bonanos, A. Z., et al. 2009, ApJL, 695, L154
Bond, H. E., Henden, A., Levay, Z. G., et al. 2003, Natur, 422, 405
Bondi, M., Pérez-Torres, M. A., Herrero-Illana, R., & Alberdi, A. 2012, A&A, 539, A134
Brown, T. M., Baliber, N., Bianco, F. B., et al. 2013, PASP, 125, 1031
Brunthaler, A., Martí-Vidal, I., Menten, K. M., et al. 2010, A&A, 516, A27
Brunthaler, A., Menten, K. M., Reid, M. J., et al. 2009, A&A, 499, L17
Chapman, N. L., Mundy, L. G., Lai, S.-P., & Evans, N. J., II 2009, ApJ, 690, 496
Cohen, M., Wheaton, W. A., & Megeath, S. T. 2003, AJ, 126, 1090
Conseil, E., Fraser, M., Inserra, C., et al. 2013, CBET, 3431
Cresci, G., Mannucci, F., della Valle, M., & Maiolino, R. 2007, A&A, 462, 927
Crockett, R. M., Eldridge, J. J., Smartt, S. J., et al. 2008, MNRAS, 391, L5
Elmegreen, B. G., Kaufman, M., Bournaud, F., et al. 2016, ApJ, 823, 26
Elmegreen, B. G., Kaufman, M., Struck, C., et al. 2000, AJ, 120, 630
Elmegreen, D. M., Kaufman, M., Elmegreen, B. G., et al. 2001, AJ, 121, 182
Ergon, M., Jerkstrand, A., Sollerman, J., et al. 2015, A&A, 580, A142
Ergon, M., Sollerman, J., Fraser, M., et al. 2014, A&A, 562, A17
Fazio, G. G., Hora, J. L., Allen, L. E., et al. 2004, ApJS, 154, 10
Filippenko, A. V., Chornock, R., Swift, B., et al. 2003, IAUC, 8159
Fitzpatrick, E. L. 1999, PASP, 111, 63
Fox, O. D., & Casper, C. 2015, IAUGA, 22, 2258045
Fox, O. D., Johansson, J., Kasliwal, M., et al. 2016, ApJL, 816, L13
Fremling, C., Sollerman, J., Taddia, F., et al. 2016, A&A, 593, A68
Fukugita, M., Ichikawa, T., Gunn, J. E., et al. 1996, AJ, 111, 1748
Gal-Yam, A., Ofek, E. O., Poznanski, D., et al. 2006, ApJ, 639, 331
Gehrz, R. D. 1988, Natur, 333, 705
Gehrz, R. D., & Ney, E. P. 1990, PNAS, 87, 4354
Gehrz, R. D., Roellig, T. L., Werner, M. W., et al. 2007, RScI, 78, 011302
Grossan, B., Spillar, E., Tripp, R., et al. 1999, AJ, 118, 705
Hamuy, M. 2003, ApJ, 582, 905
Helou, G., Kasliwal, M. M., Ofek, E. O., et al. 2013, ApJL, 778, L19
Herrero-Illana, R., Pérez-Torres, M. Á., & Alberdi, A. 2012, A&A, 540, L5
Hewett, P. C., Warren, S. J., Leggett, S. K., & Hodgkin, S. T. 2006, MNRAS, 367, 454
Hodgkin, S. T., Irwin, M. J., Hewett, P. C., & Warren, S. J. 2009, MNRAS, 394, 675
Horiuchi, S., Beacom, J. F., Kochanek, C. S., et al. 2011, ApJ, 738, 154
Horne, K. 1986, PASP, 98, 609
Humphreys, R. M., Bond, H. E., Bedin, L. R., et al. 2011, ApJ, 743, 118
Jerkstrand, A., Ergon, M., Smartt, S. J., et al. 2015, A&A, 573, A12
Jha, S., Garnavich, P., Challis, P., Kirshner, R., & Berlind, P. 1999, IAUC, 7269
Johansson, J., Goobar, A., Kasliwal, M. M., et al. 2017, MNRAS, 466, 3442
Jordi, K., Grebel, E. K., & Ammon, K. 2006, A&A, 460, 339
Kankare, E., Mattila, S., Ryder, S., et al. 2008, ApJL, 689, L97
Kankare, E., Mattila, S., Ryder, S., et al. 2012, ApJL, 744, L19
Kankare, E., Mattila, S., Ryder, S., et al. 2014, MNRAS, 440, 1052
Kasliwal, M. M., Bally, J., Masci, F., et al. 2017, arXiv:1701.01151
Kasliwal, M. M., Kulkarni, S. R., Arcavi, I., et al. 2011, ApJ, 730, 134
Kato, M., Saio, H., & Hachisu, I. 1989, ApJ, 340, 509
Kaufman, M., Elmegreen, B. G., Struck, C., et al. 2016, ApJ, 831, 161
Kelson, D. D. 2003, PASP, 115, 688
Kennicutt, R. C., Jr., Hao, C.-N., Calzetti, D., et al. 2009, ApJ, 703, 1672
Kirshner, R. P., Arp, H. C., & Dunlap, J. R. 1976, ApJ, 207, 44
Kochanek, C. S. 2011, ApJ, 741, 37
Kochanek, C. S., Adams, S. M., & Belczynski, K. 2014, MNRAS, 443, 1319
Kotak, R., Meikle, W. P. S., Farrah, D., et al. 2009, ApJ, 704, 306
Li, W., van Dyk, S. D., Filippenko, A. V., & Cuillandre, J.-C. 2005, PASP, 117, 121
Lonsdale, C. J., Diamond, P. J., Thrall, H., Smith, H. E., & Lonsdale, C. J. 2006, ApJ, 647, 185
Maeda, K., Kawabata, K., Mazzali, P. A., et al. 2008, Sci, 319, 1220
Maeda, K., Nakamura, T., Nomoto, K., et al. 2002, ApJ, 565, 405
Maiolino, R., Vanzi, L., Mannucci, F., et al. 2002, A&A, 389, 84
Mannucci, F., Maiolino, R., Cresci, G., et al. 2003, A&A, 401, 519
Mattila, S., Dahlen, T., Efstathiou, A., et al. 2012, ApJ, 756, 111
Mattila, S., Fraser, M., Smartt, S. J., et al. 2013, MNRAS, 431, 2050
Mattila, S., Greimel, R., Gerardy, C., et al. 2005a, IAUC, 8474
Mattila, S., Greimel, R., Meikle, P., et al. 2002, INGN, 6, 6
Mattila, S., & Meikle, W. P. S. 2001, MNRAS, 324, 325
Mattila, S., Meikle, W. P. S., & Greimel, R. 2004, NewAR, 48, 595
Mattila, S., Monard, L. A. G., & Li, W. 2005b, IAUC, 8473
Mattila, S., Väisänen, P., Farrah, D., et al. 2007, ApJL, 659, L9
Maund, J. R., Fraser, M., Ergon, M., et al. 2011, ApJL, 739, L37
Maund, J. R., Smartt, S. J., Kudritzki, R. P., Podsiadlowski, P., & Gilmore, G. F. 2004, Natur, 427, 129
Mazzali, P. A., Kawabata, K. S., Maeda, K., et al. 2005, Sci, 308, 1284
McLean, I. S., Steidel, C. C., Epps, H., et al. 2010, Proc. SPIE, 7735, 77351E
McLean, I. S., Steidel, C. C., Epps, H. W., et al. 2012, Proc. SPIE, 8446, 84460J
Milisavljevic, D., Fesen, R. A., Gerardy, C. L., Kirshner, R. P., & Challis, P. 2010, ApJ, 709, 1343
Miluzio, M., Cappellaro, E., Botticella, M. T., et al. 2013, A&A, 554, A127
Modjaz, M., Kirshner, R. P., Blondin, S., Challis, P., & Matheson, T. 2008, ApJL, 687, L9
Modjaz, M., & Li, W. D. 1999, IAUC, 7268
Pastorello, A., Valenti, S., Zampieri, L., et al. 2009, MNRAS, 394, 2266
Pérez-Torres, M. A., Romero-Cañizales, C., Alberdi, A., & Polatidis, A. 2009, A&A, 507, L17

Persson, S. E., Murphy, D. C., Smee, S., et al. 2013, PASP, 125, 654
Podsiadlowski, P., Hsu, J. J. L., Joss, P. C., & Ross, R. R. 1993, Natur, 364, 509
Poznanski, D., Butler, N., Filippenko, A. V., et al. 2009, ApJ, 694, 1067
Prieto, J. L., Kistler, M. D., Thompson, T. A., et al. 2008, ApJL, 681, L9
Romero-Cañizales, C., Herrero-Illana, R., Pérez-Torres, M. A., et al. 2014, MNRAS, 440, 1067
Romero-Cañizales, C., Pérez-Torres, M. A., Alberdi, A., et al. 2012, A&A, 543, A72
Sanders, N. E., Soderberg, A. M., Gezari, S., et al. 2015, ApJ, 799, 208
Schlafly, E. F., & Finkbeiner, D. P. 2011, ApJ, 737, 103
Shigeyama, T., Suzuki, T., Kumagai, S., et al. 1994, ApJ, 420, 341
Simcoe, R. A., Burgasser, A. J., Bernstein, R. A., et al. 2008, Proc. SPIE, 7014, 70140U
Simcoe, R. A., Burgasser, A. J., Schechter, P. L., et al. 2013, PASP, 125, 270
Smith, N., Andrews, J. E., van Dyk, S. D., et al. 2016, MNRAS, arXiv:1602.05203
Smith, N., Cenko, S. B., Butler, N., et al. 2012, MNRAS, 420, 1135
Sparks, W. B., Bond, H. E., Cracraft, M., et al. 2008, AJ, 135, 605
Stancliffe, R. J., & Eldridge, J. J. 2009, MNRAS, 396, 1699
Steele, T. N., Silverman, J. M., Ganeshalingam, M., et al. 2008, CBET, 1275, A1
Szczygieł, D. M., Prieto, J. L., Kochanek, C. S., et al. 2012, ApJ, 750, 77
Theureau, G., Hanski, M. O., Coudreau, N., Hallet, N., & Martin, J.-M. 2007, A&A, 465, 71
Thompson, T. A., Prieto, J. L., Stanek, K. Z., et al. 2009, ApJ, 705, 1364
Tinyanont, S., Kasliwal, M. M., Fox, O. D., et al. 2016, ApJ, 833, 231
Tsvetkov, D. Y., Volkov, I. M., Baklanov, P., Blinnikov, S., & Tuchin, O. 2009, PZ, 29 arXiv:0910.4242
Tylenda, R., Hajduk, M., Kamiński, T., et al. 2011, A&A, 528, A114
Ulvestad, J. S. 2009, AJ, 138, 1529
Vacca, W. D., Cushing, M. C., & Rayner, J. T. 2003, PASP, 115, 389
van Buren, D., Jarrett, T., Terebey, S., et al. 1994, IUAC, 5960
van Dyk, S. D., Li, W., Cenko, S. B., et al. 2011, ApJL, 741, L28
van Dyk, S. D., Zheng, W., Clubb, K. I., et al. 2013, ApJL, 772, L32
Velusamy, T., Marsh, K. A., Beichman, C. A., Backus, C. R., & Thompson, T. J. 2008, AJ, 136, 197
Werner, M. W., Roellig, T. L., Low, F. J., et al. 2004, ApJS, 154, 1
Woosley, S. E., Eastman, R. G., Weaver, T. A., & Pinto, P. A. 1994, ApJ, 429, 300
Woudt, P. A., Steeghs, D., Karovska, M., et al. 2009, ApJ, 706, 738
Yaron, O., & Gal-Yam, A. 2012, PASP, 124, 668
Yin, Q. F., & Heeschen, D. S. 1991, Natur, 354, 130